Oxygenation Catalysis by All-Inorganic, Oxidation-Resistant, Dawson-Type Polyoxoanion-Supported Transition Metal Precatalysts, $[(CH_3CN)_xM]^{n+}$ Plus $P_2W_{15}Nb_3O_{62}^{9-}$ (M = Mn^{II}, Fe^{II}, Co^{II}, Ni^{II}, Cu^{I}, Cu^{II}, Zn^{II})

Heiko Weiner, Yoshihito Hayashi, and Richard G. Finke*

Department of Chemistry, Colorado State University, Fort Collins, Colorado 80523

Received January 13, 1999

Eleven new polyoxoanion-supported transition metal acetonitrile compositions have been synthesized in 1:1, 1:2, and even a few 1:3 M^{n+} to polyoxoanion ratios; these new precatalysts were then tested for their catalytic efficacy for norbornene and cyclohexene oxygenation using $[PhIO]_n$ as the oxidant. The catalytic results identify $\{(CH_3CN)_xMn^{2+}/P_2W_{15}Nb_3O_{62}^{9-}\}$ (**1**) and $\{2(CH_3CN)_xMn^{2+}/P_2W_{15}Nb_3O_{62}^{9-}\}$ (**2**) as the best precatalysts within this new subclass of polyoxoanion-supported catalysts. The results reveal a modest ca. 14-fold rate increase for either **1** or **2** in norbornene or cyclohexene epoxidation compared to the polyoxoanion-free $[Mn^{II}(CH_3CN)_4](BF_4)_2$ solvate, kinetic results which require the presence of the $P_2W_{15}Nb_3O_{62}^{9-}$ polyoxoanion in the rate-determining step of the active catalyst. Catalyst reisolation, then IR, UV−visible, and ion-exchange resin studies (and in comparison to authentic **2** that has not undergone catalysis) provide compelling evidence that **2** is, in fact, the true catalyst. Also compared to **1** and **2** is the polyoxoanion-framework-incorporated $P_2W_{17}Mn^{III}O_{61}^{7-}$, the first such comparison of a polyoxoanion-*supported* and -*incorporated* catalyst; the results reveal, for example, a distinctive catalytic epoxidation stereochemistry for the polyoxoanion-supported vs the polyoxoanion-incorporated Mn catalysts. These experiments, only the second test of the concept of polyoxoanion-supported catalysis, provide further evidence for the conceptual distinctiveness of polyoxoanion-supported transition metals as a new subclass of all-inorganic, oxidation-resistant, polyoxoanion-based catalysts.

Introduction

Polyoxoanions[1] are attracting considerable interest as oxidation-resistant oxygenation catalysts.[2] Only one prior example exists, however, of a proven polyoxoanion-supported oxidation catalyst:[3] the cyclohexene autoxidation catalyst derived from the $P_2W_{15}Nb_3O_{62}^{9-}$-supported (1,5-COD)Ir^+ (COD = cyclooctadiene) precatalyst, $[(1,5\text{-COD})Ir{\cdot}P_2W_{15}Nb_3O_{62}]^{8-}$.[4a−e] Moreover, polyoxoanion-supported catalysts are one new member of a total of only ca. eight newer classes of polyoxoanion-based catalysts, Figure 1.[5−17] They are also discrete analogues of solid-oxide-supported, atomically dispersed transition metal catalysts.

As discrete analogues of solid-oxide-supported catalysts, polyoxoanion-supported catalysts (Figure 1, arrow 6) have the potential advantages noted previously[18] of *cis*-coordination sites, greater coordinative unsaturation, and metal mobility[19] atop the oxide surface. Possible disadvantages[20] are also conceivable for

* Corresponding author. E-mail: Rfinke@lamar.colostate.edu.

(1) (a) Pope, M. T. *Heteropoly and Isopoly Oxometalates*; Springer-Verlag: New York, 1983. (b) *Polyoxometalates: From Platonic Solids to Anti-Retroviral Activity*; Proceedings of the July 15−17, 1992 Meeting at the Center for Interdisciplinary Research in Bielefeld, Germany; Müller, A., Pope, M. T., Eds.; Kluwer Publishers: Dordrecht, The Netherlands, 1992. (c) Hill, C. L., Ed. Polyoxometalates. *Chem. Rev.* **1998**, *98*, 1−390.

(2) For recent reviews of heteropolyoxoanions in homogeneous and heterogeneous catalysis see: (a) Hill, C. L.; Prosser-McCartha, C. M. *Coord. Chem. Rev.* **1995**, *143*, 407. (b) A series of 34 recent papers in a volume devoted to polyoxoanions in catalysis: Hill, C. L. *J. Mol. Catal.* **1996**, *114*, No. 1−3, pp 1−365. (c) Mizuno, N.; Misono, M. *J. Mol. Catal.* **1994**, *86*, 319. (d) Okuhara, T.; Mizuno, N.; Misono, M. *Adv. Catal.* **1996**, *41*, 113. (e) Kozhevnikov, I. V. *Catal. Rev.—Sci. Eng.* **1995**, *37* (2), 311. (f) See also the two chapters beginning on pp 171 and 199 in a recent review article[1c] that focuses on catalysis using polyoxoanions.

(3) (a) Mizuno, N.; Lyon, D. K.; Finke, R. G. *J. Catal* **1991**, *128*, 84. (b) Mizuno, N.; Lyon, D. K.; Finke, R. G. U.S. Patent 5,250,739, October 5, 1993. (c) Weiner, H.; Trovarelli, A.; Finke, R. G. Unpublished results.

(4) (a) Finke, R. G.; Lyon, D. K.; Nomiya, K.; Sur, S.; Mizuno, N. *Inorg. Chem.* **1990**, *29*, 1784. (b) Pohl, M.; Finke, R. G. *Organometallics* **1993**, *12*, 1453. (c) Pohl, M.; Lyon, D. K.; Mizuno, N.; Nomiya, K.; Finke, R. G. *Inorg. Chem.* **1995**, *34*, 1413. (d) Nomiya, K.; Pohl, M.; Mizuno, N.; Lyon, D. K.; Finke, R. G. *Inorg. Synth.* **1997**, *31*, 186. (e) Weiner, H.; Aiken, J. D., III; Finke, R. G. *Inorg. Chem.* **1996**, *35*, 7905. Note that this 1996 paper has two typographical errors: p 7910, right-hand column, 12th line: "84% excess" should read "2% excess"; p 7910, footnote 20, 4th line: "5%" should read "0.5%". (f) FAB−MS of polyoxometalates: Trovarelli, A.; Finke, R. G. *Inorg. Chem.* **1993**, *32*, 6034. (g) Pohl, M.; Lin, Y.; Weakley, T. J. R.; Nomiya, K.; Kaneko, M.; Weiner, H.; Finke, R. G. *Inorg. Chem.* **1995**, *34*, 767. (h) Finke, R. G.; Lyon, D. K.; Nomiya, K.; Weakley, T. J. R. *Acta Crystallogr.* **1990**, *C46*, 1592.

(5) (g) Okuhara, T.; Mizuno, N.; Misono, M. *Adv. Catal.* **1996**, *41*, 113−252. (h) Mizuno, N.; Misono, M. Heteropolyanions in Catalysis. *J. Mol. Catal.* **1994**, *86*, 319, and references therein. (c) Okuhara, T.; Misono, M. In *Dynamic Processes on Solid Surfaces*; Tamaru, K., Ed.; Plenum Press: New York, 1993; Chapter 10, p 259. (d) Misono, M. Catalytic Chemistry of Solid Polyoxometalates and Their Industrial Applications. In *Polyoxometalates: From Platonic Solids to Anti-Retroviral Activity*; Proceedings of the July 15−17, 1992 Meeting at the Center for Interdisciplinary Research in Bielefeld, Germany; Müller, A., Pope, M. T., Eds.; Kluwer Publishers: Dordrecht, The Netherlands, 1992; pp 255−265.

(6) (a) Baker noted as early as 1973 that mono-metal-substituted polyoxometalates ligate the metal in a pseudo-porphyrin environment: Baker, L. C. W. *Plenary Lecture, XV International Conference on Coordination Chemistry, Proceedings*, Moscow, 1973. (b) Two lead reviews to the extensive work of metalloporphyrin-catalyzed oxidations: (i) Meunier, B. *Catal. Met. Complexes* **1994**, *17*, 1−47. (ii) Meunier, B. *Chem. Rev.* **1992**, *92*, 1411−1456. (c) For a lead reference to the work of Pope, Hill, Lyons, Neumann, and our own work, see refs 17−34 summarized in: Lyon, D. K.; Miller, W. K.; Novet, T.; Domaille, P. J.; Evitt, E.; Johnson, D. C.; Finke, R. G. *J. Am. Chem. Soc.* **1991**, *113*, 7209.

10.1021/ic990078k CCC: $18.00
Published on Web 05/07/1999

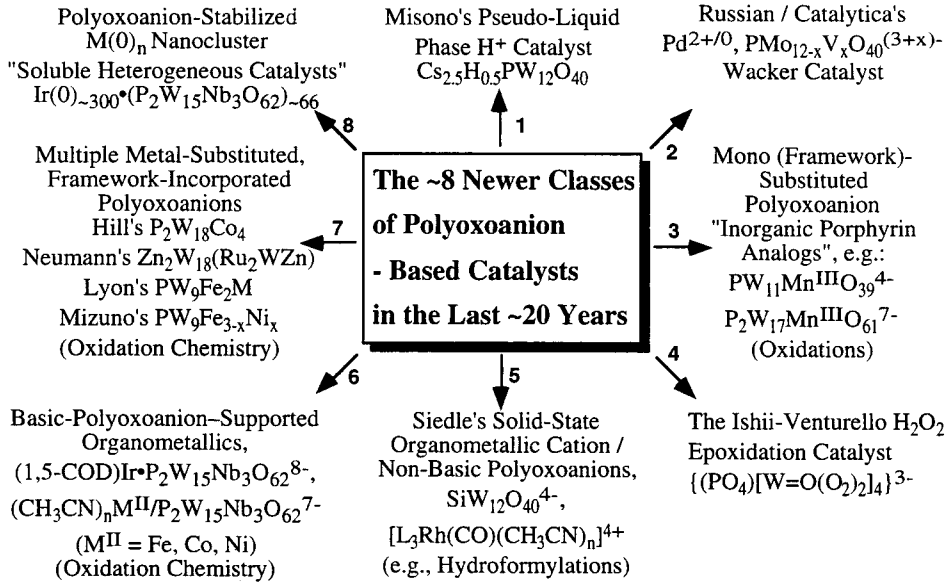

Figure 1. The eight newer classes of polyoxoanion-based catalysis in the last ca. 20 years, virtually all of which are easily identifiable by the fact that they involve *new synthetic work* and are patented, are, arguably and in our opinion: (1) Misono's pseudo-liquid-phase catalysts,[5] (2) Russian Wacker-type $Pd^{2+/0}$ and V-containing polyoxoanion catalysts (as further developed and patented by Catalytica; see p 281 elsewhere[1b]); (3) Baker-type[6a] polyoxoanion single-metal-substituted, *framework-incorporated* catalysts, such as the $PW_{11}MnO_{39}^{4-}$ or $P_2W_{17}MnO_{61}^{7-}$ "inorganic porphyrin[6b] analogue catalysts" developed by Pope, Hill, Lyons, Neumann and ourselves;[6c] (4) the Ishii−Venturello $[(PO_4)(W{=}O(O_2)_2]^{3-}$ epoxidation catalyst employing H_2O_2 and investigated mechanistically by Hill and co-workers;[7] (5) Siedle's new solid-state catalysts composed of organometallic cations plus polyoxoanions;[8] (6) polyoxoanion-*supported* catalysts;[9] (7) a rapidly developing area of *multiple-metal substituted*, framework-incorporated catalysts, such as Lyons' "PW_9Fe_2M" (M = Ni, Fe, Mn, Co, Zn) complexes[10] or Mizuno's recent work with the $PW_9Fe_{3-x}Ni_x$ complexes,[11] Hill's derivatives[12] of the $P_4W_{30}M_4$ type systems,[13] or Neumann's work with the interesting $P_2W_{18}M_4$ analogues such as[14] $Zn_2W_{18}(Mn_2ZnW)$ or $Zn_2W_{18}(Ru_2ZnW)$;[15,16] and (8) polyoxoanion-stabilized nanocluster "soluble heterogeneous catalysts".[17] A main point made apparent by this figure is that both homogeneous and heterogeneous catalysis with polyoxoanions is still a young, wide-open field for those willing to do new synthetic polyoxoanion chemistry.

polyoxoanion-supported catalysts. Hence, it is important to explore further this little-studied subclass of polyoxoanion-based catalysts. This, in turn, requires progress in the slower steps[4c] of synthesis and characterization of new polyoxoanion-supported precatalysts.

Herein we report, as only the second test of the concept of polyoxoanion-supported catalysts, the preparation of the $P_2W_{15}Nb_3O_{62}^{9-}$ polyoxoanion-supported[4e] transition metal acetonitrile complexes, $[M^{n+}(CH_3CN)_y]^{n+}$ (M^{n+} = Mn^{II}, Fe^{II}, Co^{II}, Ni^{II}, Cu^{I}, Cu^{II}, Zn^{II}; y = 4, 6) and then initial catalyst survey experiments of norbornene[21a] and cyclohexene epoxidation using the well-studied oxidant[21b] $[PhIO]_n$. Furthermore, we report the first direct comparison of a polyoxoanion-supported vs a

(7) A lead reference, one which includes references to all of the earlier work (including that original work of Ishii and Venturello, and that of the French, British, and Italian groups) is: Duncan, D. C.; Chambers, R. C.; Hecht, E.; Hill, C. L. *J. Am. Chem. Soc.* **1995**, *117*, 681.

(8) Siedle, A. R.; Gleason, W. B.; Newmark, R. A.; Skarjune, R. P.; Lyon, P. A.; Markell, C. G.; Hodgson, K. O.; Roe, A. L. *Inorg. Chem.* **1990**, *29*, 1667, and the earlier papers in this series referenced therein.

(9) (a) Mizuno, N.; Lyon, D. K.; Finke, R. G. U.S. Patent 5,250,739, Issued Oct 5, 1993. (b) Mizuno, N.; Lyon, D. K.; Finke, R. G. *J. Catal.* **1991**, *128*, 84−91. (c) Mizuno, N.; Weiner, N.; Finke, R. G. *J. Mol. Catal.* **1996**, *114*, 15−28.

(10) Elis, P. E., Jr.; Lyons, J. E. U.S. Patent 4,898,989, Feb 6, 1990

(11) Mizuno, N.; Hirose, T.; Tateishi, Iwamoto, M. *J. Mol. Catal.* **1994**, *88*, L125.

(12) (a) Hill, C. L.; Khenkin, A. M. *Mendeleev Commun.* **1993**, *4*, 140. (b) Zhang, X.; Sasaki, K.; Hill, C. L. *J. Am. Chem. Soc.* **1996**, *118*, 4809.

(13) (a) Finke, R. G.; Droege, M. W.; Domaille, P. J. *Inorg. Chem.* **l987**, *26*, 3886. (b) Weakley, T. J. R.; Finke, R. G. *Inorg. Chem.* **1990**, *29*, 1235. (c) Randall, W. J.; Droege, M. W.; Mizuno, N.; Nomiya, K.; Weakley, T. J. R., Finke R. G. *Inorg. Synth.* **1997**, *31*, 167.

(14) A paper by R. Neumann et al. is notable both for its catalytic findings, the stability of the polyoxonion catalyst to the normally structure-disrupting H_2O_2, and also for its valuable mechanistic work: Neumann, R.; Gara, M. *J. Am. Chem. Soc.* **1995**, *117*, 5066.

(15) (a) Neumann, R.; Khenkin, A. M.; Dahan, M. *Angew. Chem., Int. Ed. Engl.* **1995**, *34* , 1587. See also their subsequent full paper with the Pd^{II} and Pt^{II} analogues of the Ru^{II} complex: Neumann, R.; Alexander, M. K. *Inorg. Chem.* **1995**, *34*, 5753. (b) Neumann, R.; Dahan, M. *Nature* **1997**, *388*, 353.

(16) The *most significant reactions are, however, unevenly distributed among these classes*, with the Misono strong acid catalysis, and Ishii−Venturello H_2O_2 epoxidation chemistry, arguably among the most important advances *at this time*. One should also note that the oldest, and the (at least presently) commercially most important areas of polyoxoanions in catalysis, employ off-the-shelf, classical polyoxoanions such as $PW_{12}O_{40}^{3-}$ or $SiW_{12}O_{40}^{4-}$ for strong acid or solid-state oxidation catalysis.[5] In the H^+ catalysis area, the SiO_2−heteropoly acid inclusion complex catalysts should perhaps be included in Figure 1 (see p 184 elsewhere[1c]). Other catalytic chemistries are not included in Figure 1 because the polyoxoanions employed are not novel, although in some cases the *use* of known polyoxoanions is novel and, hence, noteworthy for that different reason [e.g., the patented, Weinstock−Hill wood pulp delignification reactions with V-substituted polyoxometalates (see p 186 elsewhere[1c])].

(17) (a) Although polyoxoanion purists might be tempted to exclude these nanocluster catalysts from the list, since the catalysis is not at the polyoxoanion itself, this would be an error. The polyoxoanion is *the* integral and crucial part of the higher stability and isolability−and the unprecedented nanocluster catalysis in solution with limited metal-particle agglomeration−exhibited by these novel "soluble heterogeneous catalysts". See: Aiken, J. D., III; Lin, Y.; Finke, R. G. *J. Mol. Catal.* **1996**, *114*, 29−51; Aiken, J. D., III; Finke, R. G. *J. Mol. Catal.* **1999**, in press (a review with 151 references titled A Review of Modern Transition-Metal Nanoclusters: Their Synthesis, Characterization, and Applications in Catalysis). In addition, the *range* of possible, albeit presently unproven, types of catalytic reactions possible by these "soluble heterogeneous catalysts" is large compared to those of any other single class of polyoxoanion-based catalysts since they potentially include many of the wide range of reactions of heterogeneous, metal-particle catalysts. (b) Lin, Y.; Finke, R. G. *J. Am. Chem. Soc.* **1994**, *116*, 8335. (c) Lin, Y.; Finke, R. G. *Inorg. Chem.* **1994**, *33*, 4891. (d) Watzky, M. A.; Finke, R. G. *J. Am. Chem. Soc.* **1997**, *119*, 10382. (e) Watzky, M. A.; Finke, R. G. *Chem. Mater.* **1997**, *9*, 3083. (f) Aiken, J. D., III; Finke, R. G. *J. Am. Chem. Soc.* **1998**, *120*, 9545.

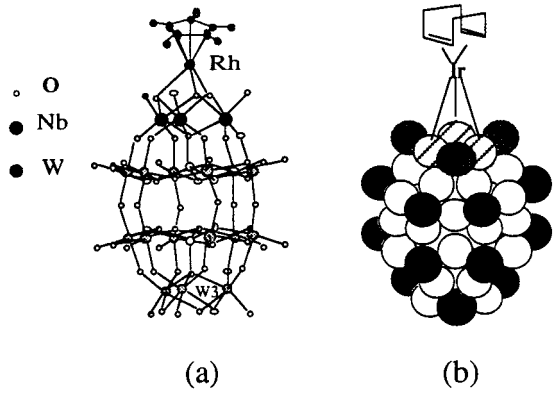

Figure 2. (a) Crystallographically determined structure of $[(C_5Me_5)Rh{\cdot}P_2W_{15}Nb_3O_{62}]^{7-}$.[4g] The Nb and W(3) atoms each are composites, $Nb_{0.5}W_{0.5}$, because the anion adopts two equally weighted orientations related by the mirror plane of a 3/*m* (D_{3h}) crystallographic site. The C_5Me_5 group lies in a plane normal to the anion C_3 axis and is disordered because of the incompatibility of its 5-fold symmetry with the C_3 axis.[4g] (b) Space-filling representation of the proposed average C_{3v} (pseudo) symmetry structure for the $[(1,5\text{-COD})Ir^+$ fragment supported on the "$Nb_3O_9^{3-}$" face of $(n\text{-}Bu_4N)_9P_2W_{15}Nb_3O_{62}$ serving as a stereochemically rigid tripodal ligand. The black circles represent terminal oxygens, the white circles are bridging oxygens, the gray circles are terminal Nb−O oxygens, and the hatched circles are the three Nb−O−Nb oxygens. The figure was generated from crystal structure parameters[4h] of $(n\text{-}Bu_4N)_9P_2W_{15}Nb_3O_{62}$ and modified using Chem 3-D. The proposed structure has been confirmed by ^1H, ^{13}C, ^{31}P, ^{17}O, and ^{183}W NMR spectroscopy as well as IR spectroscopy, sedimentation-equilibrium molecular-weight measurements, and complete elemental analysis.[4a−d]

polyoxoanion-framework-incorporated catalyst. Specifically, we compare the best precatalyst found from the above series, $\{(CH_3CN)_xMn^{2+}/P_2W_{15}Nb_3O_{62}^{9-}\}$ (**1**) to its framework-incorporated analogue,[22,23] $P_2W_{17}Mn^{III}O_{61}^{7-}$, in the catalytic tests of total epoxidation turnovers (TTOs) during 48 h and epoxidation stereochemistry, the latter using the standard probe of *cis*- and *trans*-stilbene. This comparison plus the choice of $[PhIO]_n$ as the oxidant allows, in turn, a comparison of the efficacy of $\{(CH_3CN)_xMn^{2+}/P_2W_{15}Nb_3O_{62}^{9-}\}$ (**1**), catalyzed oxygenations to the well-studied Mn^{III} porphyrins, Mn(TPP)Cl and Mn(TDCPP)Cl, since $P_2W_{17}MnO_{61}^{7-}$ was compared previously to these prototype porphyrin catalysts in studies employing $[PhIO]_n$ as the oxidant.[21b]

Results and Discussion

Spectral Titrations. To start, UV−visible spectroscopic titrations in acetonitrile were performed in order to determine the preferred composition, *at least in solution*, vide infra, of $(n\text{-}Bu_4N)_9P_2W_{15}Nb_3O_{62}$ and $[M^{n+}(CH_3CN)_y](BF_4)_n$ (M = Fe^{II}, Co^{II}, Ni^{II}, Mn^{II}, Zn^{II}, Cu^{II}, Cu^{I}; $y = 4, 6$; $n = 1, 2$), Figure 3. (The spectral changes in the UV−visible titrations are summarized in Figures S2 − S4, Supporting Information.) Characteristic oxygen-to-metal charge-transfer transitions[24] with absorption maxima around 400 nm were found for all complexes investigated, reflecting the support interaction of the transition metals with the established $Nb_3O_9^{3-}$ support site[4] in $P_2W_{15}Nb_3O_{62}^{9-}$. Cobalt shows a clean break point at 1.0 equiv of the metal solvate per equivalent of $P_2W_{15}Nb_3O_{62}^{9-}$. Interestingly, two break points are found for Mn^{II} and Fe^{II}, at 1.0 and 2.0 equiv, indicating the formation of a 1:1 M^{II} to $P_2W_{15}Nb_3O_{62}^{9-}$ (M = Mn, Fe) complex as well as a 2:1 complex at higher M^{II} to $P_2W_{15}Nb_3O_{62}^{9-}$ (M = Mn, Fe) ratios. Nickel and zinc were found to form 2:1 complexes; for Cu^{I} and Cu^{II} the formation of 2:1 and 3:1 complexes, respectively, was observed. These observations are consistent with the 3-fold axis of $P_2W_{15}Nb_3O_{62}^{9-}$ and our recent detection of "off-C_{3v} axis" isomers of $P_2W_{15}Nb_3O_{62}^{9-}$ supported transition metals; the detection of 2:1 and even 3:1 complexes had long been anticipated by us, based on Klemperer's findings of such complexes (especially for d^8, square-planar metals).[25] However, the exact structures of the multiple Zn^{2+}, Ni^{2+}, or $Cu^{+/2+}$ adducts will require that strongly diffracting single crystals be forthcoming for X-ray structural investigation.

Note that, in what follows, and given our many years of experience with synthesizing and characterizing polyoxoanions, we deliberately chose an approach in this work of (i) first doing the spectral titrations to identify the preferred M(II)/polyoxo-

(18) Finke, R. G.; Rapko, B.; Domaille, P. J. *Organometallics* **1986**, *5*, 175; see footnote 1f therein.

(19) For an example where the cation $Re(CO)_3^+$ is mobile atop the $P_2W_{15}Nb_3O_{62}^{9-}$ polyoxoanion, see: Nagata, T.; Pohl, M.; Weiner, H.; Finke, R. G. *Inorg. Chem.* **1997**, *36*, 1366.

(20) (a) The anticipated main disadvantage of polyoxoanion-*supported* catalysts, in comparison to polyoxoanion-*framework-incorporated* catalysts of the same transition metal, is that the polyoxoanion-supported catalysts may be less thermally stable or more susceptible to catalyst-degradation side reactions. Hence, catalyst lifetime is a key issue which remains to be further explored—indeed, it has been noted in the Vision 2020 report that "controlling catalyst lifetime and stability are regarded as integral to any endeavor in catalysis". [20b] (b) Vision 2020 Catalysis Report, Council of Chemical Research, March 20−21, 1997, available on the WWW (via http://www.chem.purdue.edu/v2020).

(21) (a) We deliberately chose the more reactive olefin norbornene, with its bridgehead allylic positions, for these initial survey studies in addition to the more stringent test substrate cyclohexene, with its activated allylic positions, a substrate we employed previously,[9] because of our long-term interest in finding and developing dioxygenase-type catalysts, one of the most important problems in all of oxidation catalysis. Our strategy is that this is best done, at least initially, using a substrate (such as norbornene) where allylic oxidation is deliberately suppressed so that any extant dioxygenase activity can first be *observed*, then optimized, and then extended rationally to more difficult substrates where allylic oxidation is possible (e.g., in propene). (b) We also deliberately chose $[PhIO]_n$ as the initial oxidant as this, then, allows the first comparison, of the present $\{m(CH_3CN)_xM_n^{2+}/P_2W_{15}Nb_3O_{62}^{9-}\}$ ($m = 1, 2$) catalysts in particular, to earlier work with $P_2W_{17}Mn^{III}O_{61}^{7-}$ and to Mn^{III}(porphyrin) complexes.[22] We note that this (deliberate) choice precludes most meaningful mechanistic studies which, however, are *not* a goal of the present work. Studies of other oxidants, such as *p*-cyano-*N*,*N*-dimethylaniline *N*-oxide[12b] or, better, dioxygen (the focus of our own, upcoming publications), can of couse be performed where mechanistic studies are the primary goal.

(22) (a) Lyon, D. K.; Miller, W. K.; Novet, T.; Domaille, P. J.; Evitt, E.; Johnson, D. C.; Finke, R. G. *J. Am. Chem. Soc.* **1991**, *113*, 7209. (b) Mansuy, D.; Bartoli, J.-F.; Battioni, P.; Lyon, D. K.; Finke, R. G. *J. Am. Chem. Soc.* **1991**, *113*, 7222.

(23) Polyoxoanion-framework-incorporated complexes, that is, where the metal, M, occupies the lacunary position in the polyoxoanion framework such as in the prototype complexes $PW_{11}M^{n+}O_{39}^{n-7}$ and $P_2W_{17}M^{n+}O_{61}^{n-10}$ (where $M^{n+} = Mn^{III}$, Fe^{III}, Co^{II}, Ni^{II}, and Cu^{II} among others) have been known for some time. Hence, these and other, more complicated but now also well-established structures (e.g., such as the $P_2W_{18}M_4O_{62}^{10-}$ and $P_4W_{30}M_4O_{112}^{16-}$ structures) are more widely investigated as catalysts. For lead references see the citations summarized in refs 17−34 elsewhere,[22a] and in a recent review[1c] and specialty volume,[2b] which includes the seminal works of Pope, Hill, Lyons, Neumann, as well as our own studies of $P_2W_{17}M^{n+}O_{61}^{n-10}$.

(24) (a) The assignment as a oxygen-to-metal charge-transfer band is based on the absorption range ($\lambda_{max} = 380-385$ nm; 25 970−26 320 cm^{-1}) and its intensity ($\epsilon_{max} \sim 1000$ L/(mol·cm)). See: (a) Figgis, B. N. *Introduction to Ligand Fields*; John Wiley: New York, 1966; pp 21, 245−247. (b) Hueey, J. E.; Keiter, E. A.; Keiter, R. L. *Principles of Structure and Reactivity*, 4th ed.; Harper Collins College Publishers: New York, 1993; pp 455−459. For one example of charge-transfer bands in polyoxometalates, see: Zonnevijlle, F.; Tourne, C. M.; Tourne, G. F. *Inorg. Chem.* **1982**, *21*, 2751.

(25) For example, see: (a) $\{[(1,5\text{-COD})Ir]_5(Nb_2W_4O_{19})_2\}^{3-}$; $\{[(1,5\text{-COD})Ir]_2H(Nb_2W_4O_{19})_2\}^{5-}$: Day, V. W.; Klemperer, W. G.; Main, D. J. *Inorg. Chem.* **1990**, *29*, 2345. (b) $\{[(OC)Rh]_5(Nb_2W_4O_{19})_2\}^{3-}$; $\{[(OC)Rh]_3(Nb_2W_4O_{19})_2\}^{5-}$; $\{[(OC)Ir]_2H(Nb_2W_4O_{19})_2\}^{5-}$: Klemperer, W. G.; Main, D. J. *Inorg. Chem.* **1990**, *29*, 2355.

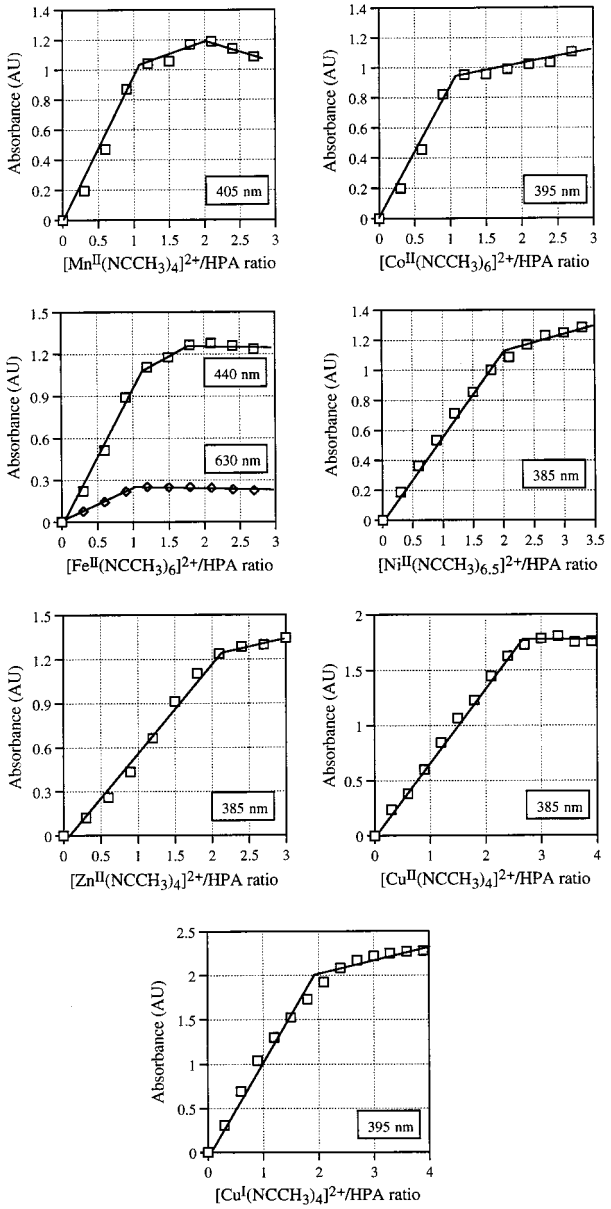

Figure 3. Plots of absorbance vs metal complex-to-polyoxoanion ratio for the $(n\text{-Bu}_4\text{N})_9\text{P}_2\text{W}_{15}\text{Nb}_3\text{O}_{62}$ heteropolyanion (HPA) with the different $[\text{M}^{n+}(\text{CH}_3\text{CN})_y](\text{BF}_4)_n$ solvates. The data were obtained using the oxygen-to-metal charge-transfer absorption[24] at ~400 nm, a band reported herein for the first time and observed only for the *supported* complexes (see Figures S2−S4, Supporting Information).

metalate stoichiometry *in solution*, *where catalysis occurs*; (ii) then synthesizing the complexes identified by the spectral titrations; (iii) then emphasizing, overall, the *catalytic* studies to identify only those complexes of true interest for subsequent time- and manpower-consuming structural characterizations; and (iv) then, and only then, beginning characterization of only the most interesting catalysts. Note that this is the appropriate, if not only viable, approach at this stage of development of polyoxoanion-supported catalysts, and if one wants to develop new oxygenation catalysts. It is an approach that adopts the "lesson of Mittach"[26] in terms of the importance of catalyst screening—even these days when catalyst design is a common theme. Indeed, the importance of catalyst screening has been modernized, and expanded in scope, with the advent of combinatorial chemisty approaches to synthesis and screening.[27]

Preparations. Eleven polyoxoanion-supported transition metal acetonitrile complexes were prepared with attention to the preferred stoichiometries uncovered via the UV−visible titrations: $\{(\text{CH}_3\text{CN})_x\text{Mn}^{2+}/\text{P}_2\text{W}_{15}\text{Nb}_3\text{O}_{62}^{9-}\}$, **1**; $\{2(\text{CH}_3\text{CN})_x\text{Mn}^{2+}/\text{P}_2\text{W}_{15}\text{Nb}_3\text{O}_{62}^{9-}\}$, **2**; $\{(\text{CH}_3\text{CN})_x\text{Co}^{2+}/\text{P}_2\text{W}_{15}\text{Nb}_3\text{O}_{62}^{9-}\}$, **3**; $\{2(\text{CH}_3\text{CN})_x\text{Co}^{2+}/\text{P}_2\text{W}_{15}\text{Nb}_3\text{O}_{62}^{9-}\}$, **4**; $\{(\text{CH}_3\text{CN})_x\text{Fe}^{2+}/\text{P}_2\text{W}_{15}\text{Nb}_3\text{O}_{62}^{9-}\}$, **5**; $\{2(\text{CH}_3\text{CN})_x\text{Fe}^{2+}/\text{P}_2\text{W}_{15}\text{Nb}_3\text{O}_{62}^{9-}\}$, **6**; $\{2(\text{CH}_3\text{CN})_x\text{Ni}^{2+}/\text{P}_2\text{W}_{15}\text{Nb}_3\text{O}_{62}^{9-}\}$, **7**; $\{2(\text{CH}_3\text{CN})_x\text{Cu}^{2+}/\text{P}_2\text{W}_{15}\text{Nb}_3\text{O}_{62}^{9-}\}$, **8**; $\{3(\text{CH}_3\text{CN})_x\text{Cu}^{2+}/\text{P}_2\text{W}_{15}\text{Nb}_3\text{O}_{62}^{9-}\}$, **9**; $\{2(\text{CH}_3\text{CN})_x\text{Cu}^{+}/\text{P}_2\text{W}_{15}\text{Nb}_3\text{O}_{62}^{9-}\}$, **10**; and $\{2(\text{CH}_3\text{CN})_x\text{Zn}^{2+}/\text{P}_2\text{W}_{15}\text{Nb}_3\text{O}_{62}^{9-}\}$, **11**. All preparations were carried out according to eq 1 and in

$$(n\text{-Bu}_4\text{N})_9\text{P}_2\text{W}_{15}\text{Nb}_3\text{O}_{62} + m[\text{M}^{n+}(\text{NCCH}_3)_y](\text{BF}_4)_n \xrightarrow[2\text{ h, }25\text{ °C}]{\text{CH}_3\text{CN, N}_2} (n\text{-Bu}_4\text{N})_{(9-n\times m)}\{m[(\text{CH}_3\text{CN})_x\text{M}^{n+}]/\text{P}_2\text{W}_{15}\text{Nb}_3\text{O}_{62}^{9-}\} + (n \times m)(n\text{-BF}_4\text{N})\text{BF}_4 \quad (1)$$

a nitrogen atmosphere drybox (<1 ppm oxygen), and all complexes were obtained as their all-tetrabutylammonium salts (n-Bu_4N^+).

Initially, we attempted to subject the 1:1 $(\text{CH}_3\text{CN})_x\text{M}^{n+}$ to $\text{P}_2\text{W}_{15}\text{Nb}_3\text{O}_{62}^{9-}$ complexes of Mn^{II}, Co^{II} and Fe^{II} (**1**, **3**, and **5**, respectively) to our typical ethyl acetate/acetonitrile precipitation[4,19] to remove the 2 equiv of n-$\text{Bu}_4\text{N}^+\text{BF}_4^-$ produced in the synthesis (eq 1). However, analytical data (available in the Supporting Information) revealed that the attempted precipitation of **1**, **3**, and **5** from ethyl acetate/acetonitrile induced the exchange reaction shown in eq 2, followed by the selective

$$2\{(\text{CH}_3\text{CN})_x\text{M}^{2+}/\text{P}_2\text{W}_{15}\text{Nb}_3\text{O}_{62}^{9-}\} \underset{\text{induced precipitation}}{\overset{\text{EtOAc/CH}_3\text{CN}}{\rightleftharpoons}} \{2(\text{CH}_3\text{CN})_x\text{M}^{2+}/\text{P}_2\text{W}_{15}\text{Nb}_3\text{O}_{62}^{9-}\}\downarrow + \text{P}_2\text{W}_{15}\text{Nb}_3\text{O}_{62}^{9-} \quad (2)$$

precipitation of the less soluble 2:1 $\{2(\text{CH}_3\text{CN})_x\text{M}^{2+}/\text{P}_2\text{W}_{15}\text{Nb}_3\text{O}_{62}^{9-}\}$ (M = Mn, Co, Fe) complexes. Hence, by necessity complexes **1**, **3**, and **5** had to be isolated by simply removing the solvent under vacuum and without further manipulation. However, complexes **2**, **4**, and **6**−**11** could be, and therefore were, purified by reprecipation from $\text{CH}_3\text{CN/EtOAc/Et}_2\text{O}$.

(26) (a) A. Mittasch, in 1909, is generally credited for the strategy of extensive catalyst screening to invent new catalyst compositions. Specifically, his ca. 6500 screenings of ca. 2500 catalysts led to the still largely unchanged industrial NH_3 synthesis catalyst (see ref 1 and the discussion of this provided by Ertl elsewhere[26b]). It is a nontrivial observation that this strategy is still important today in catalysis, not to mention modern versions of this strategy in the form of combinatorial synthesis and screening.[27] (b) Ertl, G. *Angew. Chem., Int. Ed. Engl.* **1990**, *29*, 1219.

(27) (a) Two (thematic volume) reviews on combinatorial chemistry: Szostak, J. (guest editor) *Chem. Rev.* **1997**, *97*, 347−510 (Combinatorial Chemistry; eight separate chapters); *Acc. Chem. Res.* **1996**, *29*, 112−170 (Special Issue: Combinatorial Chemistry; six separate chapters). (b) For a recent lead reference to some of the issues and needs in combinatorial chemistry applied to catalysis, see: Cooper, A. C.; McAlexander, L. H.; Lee, D.-H.; Torres, M. T.; Crabtree, R. H. *J. Am. Chem. Soc.* **1998**, *120*, 9971 (and refs 1a−d therein). (c) For an early attempt to do combinatorial chemistry in polyoxoanion catalysis which, however, screened only a 3 × 13 array of catalyst compositions, see: Hill, C. L.; Damico Gall, R. *J. Mol. Catal. A: Chem.* **1996**, *114*, 103. (d) For a polymer-based, combinatorially developed synthetic phosphatase catalyst see: Menger, F. M.; Eliseev, A. V.; Migulin, V. A. *J. Org. Chem.* **1995**, *60*, 6666. That work also makes apparent the limitations of at least some combinatorially discovered catalysts. The true identity of the best catalyst will, the authors note, likely never be known, so that subsequent rational improvements of that catalyst, nor principles from its composition, structure or mechanism, will never be known. Another issue is the extent to which the results from catalysts discovered combinatorially are repeatable, either in the same labs or in different labs.

A typical preparation for the 11 new complexes, with adjustments in the isolation and purification procedure as required for different complexes, is as follows. In the drybox 500 mg (0.08 mmol) of $(n\text{-}Bu_4N)_9P_2W_{15}Nb_3O_{62}$ was dissolved in 5 mL of acetonitrile and placed in a 25 mL round-bottom flask, followed by dropwise addition over 2 min of the required amount of the $[M^{n+}(CH_3CN)_y](BF_4)_n$ complex dissolved in 1 mL of acetonitrile. The resulting clear, homogeneous solution was then stirred for 2 h. Complexes **1**, **3**, and **5** were isolated at this point simply by removing the solvent in vacuo, then storing the resultant solids in a drybox. For the complexes **2**, **4**, and **6**−**11**, after the acetonitrile reaction solvent (eq 1) was removed under vacuum at room temperature, first 0.5 mL of acetonitrile and then 0.5 mL of ethyl acetate were added. The mixture was then transferred with a plastic pipet into a 10 mL glass vial containing a 1 cm magnetic stir bar. Next, 4 mL of dry diethyl ether was added to the mixture under vigorous stirring, causing the formation of a fine (in some cases oily) precipitate. The crude materials **2**, **4**, and **6**−**11** still contain ∼0.4 equiv of $n\text{-}Bu_4N^+BF_4^-$ at this stage (determined by ^{19}F NMR for the diamagnetic Zn^{II} complex, **11**; e.g., see Figure S8, Supporting Information; the ^{19}F NMR chemical shifts are identical to those for free BF_4^- and thus indicate, as expected, no interaction of any residual BF_4^- with the supported Zn^{II}).[28] The materials from each synthesis were then collected on a 15 mL medium glass frit and rinsed twice with 3 mL of ethyl acetate. The resultant washed solids were then redissolved in 0.5 mL of acetonitrile, and 0.5 mL of ethyl acetate was added over 2 min. The polyoxometalates **2**, **4**, and **6**−**11** were then reprecipitated by adding the solution dropwise over ca. 2 min to 60 mL of dry ethyl acetate under vigorous stirring. At this point the isolated yields of crude materials averaged 50−80%. (Specific isolated yields are given in the Experimental Section.) After 30 min the precipitate was collected on a 15 mL medium glass frit, redissolved again in 0.5 mL of acetonitrile and ethyl acetate, and the reprecipitation procedure was repeated. The final products **2**, **4**, and **6**−**11** contained ≤0.5 equiv (≤2.7% total by weight) of $n\text{-}Bu_4N^+BF_4^-$ by ^{19}F NMR (e.g., see Figure S8 of the Supporting Information for the spectrum for the diamagnetic Zn^{II} complex, **11**). After the two reprecipitations the overall yields are about 38−60%. The composition of the isolated products were confirmed by elemental analysis and IR, plus FAB-MS for the Mn^{II}, Co^{II}, and Fe^{II} complexes. Positive-ion and negative-ion FAB-MS spectra of **2**, **4**, and **6** are provided in Figures S10−S13 as Supporting Information, although they proved relatively uninformative as (a result not atypical for most of the polyoxoanion-*supported* transition metal complexes we have examined to date by FAB-MS[4f]).

Catalytic Survey Experiments: Norbornene and Cyclohexene Epoxidation. The 11 polyoxoanion-supported precatalysts were examined for their efficacy in norbornene and cyclohexene epoxidation using $[PhIO]_n$ in acetonitrile,[29] eq 3;

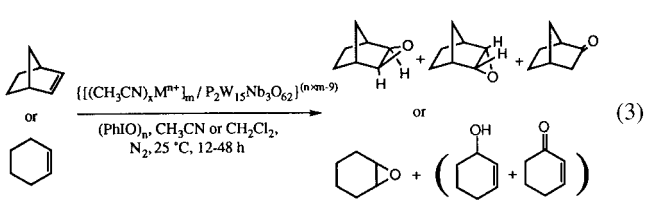

(3)

several key controls were also performed.

First, as expected, control reactions using either $\{2(CH_3CN)_xZn^{2+}/P_2W_{15}Nb_3O_{62}^{9-}\}$ (**11**) or the parent polyoxoanion alone, $P_2W_{15}Nb_3O_{62}^{9-}$ exhibited no catalytic activity. Second,

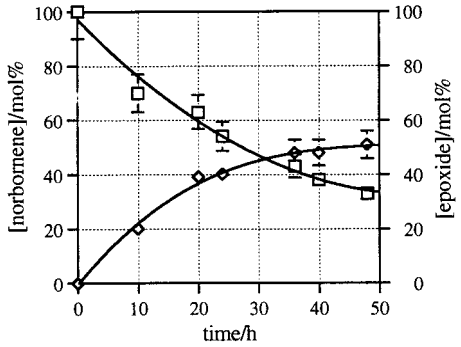

Figure 4. Time course of norbornene oxygenation in acetonitrile at 25 °C by $[PhIO]_n$ in the presence of the best catalyst, $\{2(CH_3CN)_xMn^{2+}/P_2W_{15}Nb_3O_{62}^{9-}\}$ (**2**). Formation of 22% (41.8 μmol) of epoxide (right *y* axis) at ca. 24% conversion of norbornene (left *y* axis) was found after 12 h.

controls using the *unsupported* (polyoxoanion-free) transition metal acetonitrile solvates[30] $[M^{2+}(CH_3CN)_y](BF_4)_2$ (M^{2+} = Mn, Fe, Co; y = 4, 6) exhibited both lower conversion (<5%) and lower catalytic efficacy than the polyoxoanion-supported $[M^{n+}(CH_3CN)_x]^{n+}$ complexes [total turnovers (TTOs), in 48 h, of 2.0 (Mn), 2.1 (Co), and 1.7 (Fe) in norbornene epoxidation; 1.7 (Mn), 0.9 (Co), and 0.8 (Fe) in cyclohexene epoxidation]. Poorer norbornene oxygenation selectivity is also observed for the polyoxoanion-free $[M^{n+}(CH_3CN)_x]^{n+}$ solvates [80% of *exo*-epoxide and a sizable percentage, 20%, of the ketone, norcamphor; mass balance = 90(±10)%]. These lower activity and poorer selectivity results with the $[M^{n+}(CH_3CN)_x]^{n+}$ solvates alone are fully consistent with Valentine and co-workers' results for these same catalysts [and also for the simple Lewis acid (e.g., Zn^{II} or Al^{III}) catalysts that they examined[30]].

With the above controls in hand, the polyoxoanion-supported complexes, $\{m(CH_3CN)_xM^{n+}/P_2W_{15}Nb_3O_{62}^{9-}\}$, ($M^{n+}$ = Mn^{2+}, Fe^{2+}, Co^{2+}, m = 1, 2; M^{n+} = Cu^{2+}, m = 2, 3; M^{n+} = Ni^{2+}, Zn^{2+}, Cu^{+}, m = 2) were examined next. Time courses for norbornene epoxidation, Figure 4, and cyclohexene epoxidation, Figure 5, using the Mn^{II} supported precatalyst, $\{2(CH_3CN)_xMn^{2+}/P_2W_{15}Nb_3O_{62}^{9-}\}$ (**2**), show the formation of the corresponding epoxides. A summary of the total yields of epoxide for norbornene and cyclohexene oxygenation after 12, 36, and 48 h is provided in Tables 1 and 2.

For the polyoxoanion-supported complexes, the relative catalytic efficacys for norbornene and cyclohexene epoxidations

(28) A control experiment was performed to test the solubility of the remaining 2 equiv of $Bu_4N^+BF_4^-$ in the acetonitrile/ethyl acetate solvent: 60 mg (1.82×10^{-4} mol, 2.28 equiv) of $Bu_4N^+BF_4^-$ was dissolved in 0.5 mL of acetonitrile using a 5 mL glass vial. Then, 0.5 mL of ethyl acetate was added resulting in a clear and homogeneous solution; the addition of 4 mL of dry diethyl ether to the acetonitrile/ethyl acetate mixture did not produce any insoluble $Bu_4N^+BF_4^-$ or other material. The procedure was then repeated using 60 mg of $Bu_4N^+BF_4^-$ *and* 500 mg of $(n\text{-}Bu_4N)_9P_2W_{15}Nb_3O_{62}$ starting material. Approximately 400 mg (80%) of the $(n\text{-}Bu_4N)_9P_2W_{15}Nb_3O_{62}$ was recovered, after two reprecipitations from a acetonitrile/ethyl acetate (0.5 mL/0.5 mL) mixture and 60 mL ethyl acetate (see above-described procedure for details), for an isolated yield of 288 mg (72%). ^{19}F NMR showed that only ca. 0.11 equiv of $Bu_4N^+BF_4^-$ remained in the recovered control experiment sample of $(n\text{-}Bu_4N)_9P_2W_{15}Nb_3O_{62}$.

(29) Note that the general, overall stoichiometry with $[PhIO]_n$ as oxidant is well established to be the sum of what one can formally consider as three parallel reactions, epoxidation (a) and two PhIO disproportionation reactions (b, c): (a) olefin + $(a + 2b + 2c)$PhIO → (a) epoxide + (b) $PhIO_2$ + (c) O_2 + $(a + 2b + 2c)$PhI.

(30) (a) VanAtta, R. B.; Franklin, C. C.; Valentine, J. S. *Inorg. Chem.* **1984**, *23*, 4123. (b) Nam, W.; Valentine, J. S. *J. Am. Chem. Soc.* **1990**, *112*, 4977. (c) Yang, Y.; Diederich, F.; Valentine, J. S. *J. Am. Chem. Soc.* **1990**, *112*, 7826.

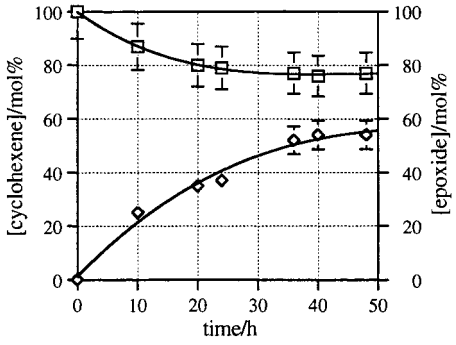

Figure 5. Time course of cyclohexene oxygenation in acetonitrile at 25 °C by $[PhIO]_n$ in the presence of the best catalyst, $\{2(CH_3CN)_xMn^{2+}/P_2W_{15}Nb_3O_{62}^{9-}\}$ (**2**). The formation of 21% (23.5 μmol) of epoxide (right *y* axis) at ca. 11% conversion of cyclohexene (left *y* axis) was found after 12 h.

in acetonitrile are shown in Figure 6, top and bottom, respectively. A comparison of total turnovers (TTOs) is provided in Figure 7. The resultant catalytic efficiencies, according to the data in either Figure 6 or 7, are the following: $\{(CH_3CN)_xMn^{2+}/P_2W_{15}Nb_3O_{62}^{9-}\} \approx \{2(CH_3CN)_xMn^{2+}/P_2W_{15}Nb_3O_{62}^{9-}\} > \{(CH_3CN)_xCo^{2+}/P_2W_{15}Nb_3O_{62}^{9-}\} \approx \{2(CH_3CN)_xCo^{2+}/P_2W_{15}Nb_3O_{62}^{9-}\} \gg \{(CH_3CN)_xFe^{2+}/P_2W_{15}Nb_3O_{62}^{9-}\} \approx \{2(CH_3CN)_xFe^{2+}/P_2W_{15}Nb_3O_{62}^{9-}\} > \{2(CH_3CN)_xCu^{2+}/P_2W_{15}Nb_3O_{62}^{9-}\} > \{3(CH_3CN)_xCu^{2+}/P_2W_{15}Nb_3O_{62}^{9-}\} \approx \{2(CH_3CN)_xNi^{2+}/P_2W_{15}Nb_3O_{62}^{9-}\} \approx \{2(CH_3CN)_xCu^{+}/P_2W_{15}Nb_3O_{62}^{9-}\} > \{2(CH_3CN)_xZn^{2+}/P_2W_{15}Nb_3O_{62}^{9-}\} \gg P_2W_{15}Nb_3O_{62}^{9-} \approx 0$ (0.001 TTOs). A very similar trend was found for cyclohexene epoxidations in acetonitrile (Figure 6, bottom; see also Figure 7): $\{(CH_3CN)_xMn^{2+}/P_2W_{15}Nb_3O_{62}^{9-}\} \approx \{2(CH_3CN)_xMn^{2+}/P_2W_{15}Nb_3O_{62}^{9-}\} > \{(CH_3CN)_xCo^{2+}/P_2W_{15}Nb_3O_{62}^{9-}\} \approx \{2(CH_3CN)_xCo^{2+}/P_2W_{15}Nb_3O_{62}^{9-}\} \gg \{(CH_3CN)_xFe^{2+}/P_2W_{15}Nb_3O_{62}^{9-}\} \approx \{2(CH_3CN)_xFe^{2+}/P_2W_{15}Nb_3O_{62}^{9-}\} > \{2(CH_3CN)_xCu^{2+}/P_2W_{15}Nb_3O_{62}^{9-}\} \approx \{3(CH_3CN)_xCu^{2+}/P_2W_{15}Nb_3O_{62}^{9-}\} \approx \{2(CH_3CN)_xNi^{2+}/P_2W_{15}Nb_3O_{62}^{9-}\} \approx \{2(CH_3CN)_xCu^{+}/P_2W_{15}Nb_3O_{62}^{9-}\} > \{2(CH_3CN)_xZn^{2+}/P_2W_{15}Nb_3O_{62}^{9-}\} \gg P_2W_{15}Nb_3O_{62}^{9-} \approx 0$. Lower rates of norbornene oxygenation were found in dichloromethane as solvent, apparently reflecting the lower solubility[31] of both the $[PhIO]_n$ and the catalysts in CH_2Cl_2 as compared to CH_3CN, Figure 8. However, the best catalytic activity is observed for the manganese(II) polyoxoanion-supported complexes, $\{(CH_3CN)_xMn^{2+}/P_2W_{15}Nb_3O_{62}^{9-}\}$ (**1**) and $\{2(CH_3CN)_xMn^{2+}/P_2W_{15}Nb_3O_{62}^{9-}\}$ (**2**).

The polyoxoanion-supported complexes produce *exo*-2,3-epoxynorbornane selectively (>98%) with only trace amounts (<2%) of the ketone, norcamphor (recall eq 3), at a mass balance $>80 \pm 10\%$. The highest observed activity for both norbornene and cyclohexene epoxidation was found for the manganese(II) complex $\{2(CH_3CN)_xMn^{2+}/P_2W_{15}Nb_3O_{62}^{9-}\}$ (**2**) (TTOs = 27.5 for norbornene, 20.2 for cyclohexene, respectively, cf. Tables 1 and 2, Figure 7). The highest activity for the Mn complex parallels the analogous results observed for both the polyoxoanion-incorporated manganese(III) analogue, $P_2W_{17}Mn^{III}O_{61}^{7-}$, and the well-established Mn^{III}(tetraphenylporphyrin; TPP) catalysts.[22b] The framework-incorported Mn^{III} catalyst $P_2W_{17}Mn^{III}O_{61}^{7-}$ is ca. 1.6-fold more active in norbornene oxygenation than the supported Mn^{II} catalyst $\{(CH_3CN)_xMn^{2+}/P_2W_{15}Nb_3O_{62}^{9-}\}$ (**1**), at least under our conditions and for the $P_2W_{15}Nb_3O_{62}^{9-}$ polyoxoanion-support system. However, an equally if not more important result is that the $P_2W_{15}Nb_3O_{62}^{9-}$ polyoxoanion's presence results in a *14-fold rate increase* (i.e., vs the simple $[Mn^{II}(CH_3CN)_4](BF_4)_2$ solvate). Although a modest rate increase, that increase means, in turn, that the *concept* of polyoxoanion-supported catalysts is further fortified.[3,4]

Stereochemical Studies. The stereochemistry of *cis*- and *trans*-stilbene oxidation for the best precatalysts, $\{(CH_3CN)_xMn^{2+}/P_2W_{15}Nb_3O_{62}^{9-}\}$ (**1**) and $\{2(CH_3CN)_xMn^{2+}/P_2W_{15}Nb_3O_{62}^{9-}\}$ (**2**), has also been determined for a reaction time of 24 h. The key results are as follows: (i) a 21−23% conversion of *cis*-stilbene to a 4:6 (0.67) ratio of *cis*- to *trans*-stilbene oxide is observed [0.68 for $\{(CH_3CN)_xMn^{2+}/P_2W_{15}Nb_3O_{62}^{9-}\}$ (**1**) and an experimentally identical 0.66 for the 2:1 complex, $\{2(CH_3CN)_xMn^{2+}/P_2W_{15}Nb_3O_{62}^{9-}\}$ (**2**)], Table 3; (ii) a 5% *cis*-to-*trans* isomerization of *cis*-stilbene occurs during the 24 h [4.8% for $\{(CH_3CN)_xMn^{2+}/P_2W_{15}Nb_3O_{62}^{9-}\}$ (**1**) and equivalent 5.2% for the 2:1 complex, $\{2(CH_3CN)_xMn^{2+}/P_2W_{15}Nb_3O_{62}^{9-}\}$ (**2**)]; and (iii) approximately 37% benzaldehyde is also observed [37% for $\{(CH_3CN)_xMn^{2+}/P_2W_{15}Nb_3O_{62}^{9-}\}$ (**1**) and an equivalent 36% for the 2:1 complex, $\{2(CH_3CN)_xMn^{2+}/P_2W_{15}Nb_3O_{62}^{9-}\}$ (**2**)]. The stereochemistry of the incorporated Mn^{III} analogue, $P_2W_{17}Mn^{III}O_{61}^{7-}$, was also examined for comparison and under the same condition; the results reveal the following: (iv) a ca. 2-fold higher, 55% conversion of *cis*-stilbene is seen with a much higher *cis*- to *trans*-stilbene oxide ratio of 2.3), Table 3; and (v) a significantly higher 42% *cis*-to-*trans* isomerization of *cis*-stilbene oxidation is observed. In the case of *trans*-stilbene, both precatalysts are slow (≤10% conversion each), with only traces of benzaldehyde side product being seen. A key point here is the heretofore untested and thus unobserved *difference* between the incorporated and supported catalysts: polyoxoanion-*supported* catalysts do indeed behave as a distinct subclass of polyoxoanion-based catalysts.[32]

Further Data on the Polyoxoanion-Supported Catalysts. Several notes are in order here about the formulations of these complexes. First, the elemental analyses of the *isolated* solids indicate that, not surprisingly,[33] the volatile CH_3CN is removed under the isolation and vaccum drying (40 °C, 10 mmHg) prior to the analyses (i.e., $x \sim 0$ in $\{m(CH_3CN)_xM^{n+}/P_2W_{15}Nb_3O_{62}^{9-}\}$. However, titration of the isolated $\{(CH_3CN)_xCo^{2+}/P_2W_{15}Nb_3O_{62}^{9-}\}$ (**3**) analogue with either CH_3CN or *N*-methylamidazole in 1,2-dichloroethane shows a break point at $x \approx 3CH_3CN$; hence, we have retained *x* (i.e., $x > 0$) in the above general formula, especially for the complexes in CH_3CN solution. [Interestingly, either pyridine or *p*-(dimethylamino)-pyridine show approximate break points at 1 equiv of pyridine per equivalent of $\{(CH_3CN)_xCo^{2+}/P_2W_{15}Nb_3O_{62}^{9-}\}$ (**3**), an observation which was not investigated further but may reflect the greater steric bulk of the pyridine ligands.] Second, it is

(31) The solubility of $[PhIO]_n$ in CH_3CN and CH_2Cl_2 was determined experimentally: 2 mL of solvent was saturated with 65 mg of $[PhIO]_n$ by stirring the suspensions under argon for 45 min. The mixtures were then filtered, 1 mL aliquots were evaporated to dryness at room temperature, and the resultant solid was weighed. The solubility of $[PhIO]_n$ in CH_3CN is ca. 6.8 g/L (3.1×10^{-2} M), and in CH_2Cl_2 it is ca. 1.6 g/L (2.3×10^{-3} M).

(32) Note here the difference between the manganese oxidation states in the Mn^{III} incorporated vs the Mn^{II} supported forms of at least the *precatalysts*. However, it is highly likely that, despite the specific oxidation state of the precatalyst, during multiple turnovers and in the presence of excess oxidant, the most stable or most active Mn oxidation state—but still not necessarily an identical oxidation state—is formed in each case. That is, the preferred *catalytic* oxidation state is likely achieved in each complex regardless if one starts with the Mn^{II} or Mn^{III} precatalyst, and for this reason we chose for this initial comparison the known, isolated, and fully characterized $P_2W_{17}Mn^{III}O_{61}^{7-}$.

(33) A loss of weakly bound acetonitrile ligands during drying procedures has previously been observed for related polyoxometalates, e.g., $[Rh(CH_3CN)CO(PPh_3)_2]_n[EW_{12}O_{40}]$ (E = P, $n = 3$; E = Si, $n = 4$). See: Strauss, S. H. *Chem. Rev.* **1993**, *93*, 927 (see p 937 and ref 118 therein).

Table 1. Epoxidation of Norbornene in Acetonitrile with $[PhIO]_n$ as Oxidant[a] at 25 °C and under 1 atm Nitrogen Using the Polyoxoanion-Supported Transition-Metal Catalysts

	epoxide yield (μmol) [and % yield in selected cases based on the limiting reagent, $[PhIO]_n$]		
precatalyst	12 h	36 h	48 h
$\{(CH_3CN)_xMn^{2+}/P_2W_{15}Nb_3O_{62}^{9-}\}$	27 [8.9%][b]	68 [22.9%][b]	62 [21%][b]
$\{2(CH_3CN)_xMn^{2+}/P_2W_{15}Nb_3O_{62}^{9-}\}$	22 [7.5%]	69 [23.1%]	67 [23%]
$\{(CH_3CN)_xFe^{2+}/P_2W_{15}Nb_3O_{62}^{9-}\}$	5.5	8.5	8.8
$\{2(CH_3CN)_xFe^{2+}/P_2W_{15}Nb_3O_{62}^{9-}\}$	5.4	8.4	9.0
$\{(CH_3CN)_xCo^{2+}/P_2W_{15}Nb_3O_{62}^{9-}\}$	23	46	46
$\{2(CH_3CN)_xCo^{2+}/P_2W_{15}Nb_3O_{62}^{9-}\}$	25	45	48
$\{2(CH_3CN)_xNi^{2+}/P_2W_{15}Nb_3O_{62}^{9-}\}$	2.1	3.2	3.6
$\{2(CH_3CN)_xCu^{2+}/P_2W_{15}Nb_3O_{62}^{9-}\}$	3.6	5.7	5.8
$\{3(CH_3CN)_xCu^{2+}/P_2W_{15}Nb_3O_{62}^{9-}\}$	3.9	4.2	4.8
$\{2(CH_3CN)_xCu^{+}/P_2W_{15}Nb_3O_{62}^{9-}\}$	2.2	2.9	3.1
$\{2(CH_3CN)_xZn^{2+}/P_2W_{15}Nb_3O_{62}^{9-}\}$	1.1	1.0	1.1
$(n\text{-}Bu_4N)_9P_2W_{15}Nb_3O_{62}$	trace	1.0	1.1
no catalyst	—	trace	trace

[a] Reaction conditions: acetonitrile, 3 mL; catalyst, 15 mg (2.5 μmol); [PhIO], 47.5 mg (216 μmol); norbornene, 28 mg (298 μmol); N_2; 25 °C. GLC conditions: Carbowax; initial temperature, 50 °C; initial time, 3 min; temperature-ramped 10°/min to a 160 °C final temperature; injector temperature, 200 °C; detector (FID) temperature, 200 °C. [b] A control of adding 8.2 mg (ca. 10 equiv) of $n\text{-}Bu_4N^+BF_4^-$ to an otherwise identical run with this catalyst had, as expected, no effect. (This control was done since complexes **1**, **3**, and **5** have 2 equiv of $n\text{-}Bu_4N^+BF_4^-$ that cannot be removed by the usual reprecipitation and purification process; see the main text.)

Table 2. Epoxidation of Cyclohexene in Acetonitrile with $[PhIO]_n$ as Oxidant[a] at 25 °C and under 1 atm Nitrogen Using the Polyoxoanion-Supported Transition-Metal Catalysts

	epoxide yield (μmol) [and % yield in selected cases based on the limiting reagent, $[PhIO]_n$]		
precatalyst	12 h	36 h	48 h
$\{(CH_3CN)_xMn^{2+}/P_2W_{15}Nb_3O_{62}^{9-}\}$	20 [4.0%]	38 [7.6%]	49 [9.8%]
$\{2(CH_3CN)_xMn^{2+}/P_2W_{15}Nb_3O_{62}^{9-}\}$	18 [3.7%]	38 [7.7%]	51 [10%]
$\{(CH_3CN)_xFe^{2+}/P_2W_{15}Nb_3O_{62}^{9-}\}$	4.0	5.2	6.2
$\{2(CH_3CN)_xFe^{2+}/P_2W_{15}Nb_3O_{62}^{9-}\}$	4.4	5.6	6.5
$\{(CH_3CN)_xCo^{2+}/P_2W_{15}Nb_3O_{62}^{9-}\}$	19	25	28
$\{2(CH_3CN)_xCo^{2+}/P_2W_{15}Nb_3O_{62}^{9-}\}$	18	25	28
$\{2(CH_3CN)_xNi^{2+}/P_2W_{15}Nb_3O_{62}^{9-}\}$	2.2	2.8	3.4
$\{2(CH_3CN)_xCu^{2+}/P_2W_{15}Nb_3O_{62}^{9-}\}$	2.0	2.9	3.6
$\{3(CH_3CN)_xCu^{2+}/P_2W_{15}Nb_3O_{62}^{9-}\}$	3.3	3.9	4.1
$\{2(CH_3CN)_xCu^{+}/P_2W_{15}Nb_3O_{62}^{9-}\}$	1.1	1.5	1.6
$\{2(CH_3CN)_xZn^{2+}/P_2W_{15}Nb_3O_{62}^{9-}\}$	0.6	0.9	1.0
$(n\text{-}Bu_4N)_9P_2W_{15}Nb_3O_{62}$	trace	trace	1.2
no catalyst	trace	trace	1.2

[a] Reaction conditions: acetonitrile, 6 mL; catalyst, 15 mg (2.5 μmol); [PhIO], 47.5 mg (216 μmol); cyclohexene, 50 μL (494 μmol); N_2; 25 °C. GLC conditions: Carbowax; initial temperature, 50 °C; initial time, 3 min; temperature-ramped 10°/min to a 160 °C final temperature; injector temperature, 200 °C; detector (FID) temperature, 200 °C.

useful to recall that a range of preferred coordination numbers and geometries are represented in the $M^{n+}(CH_3CN)_x^{n+}$ complexes added to the polyoxoanion [from 4 to 6 coordinate, and from tetrahedral (Cu^I), square planar (Cu^{II}, Ni^{II}), to octahedral (Fe^{II}, Mn^{II}, Co^{II}) geometries, depending upon the metal, d^n configuration, and ligand set]. Hence, one does not expect every metal cation to favor the facial, κ_3-O-support site presented by the "Nb_3O_9" cap in $P_2W_{15}Nb_3O_{62}^{9-}$ (and its inherent preference for T_d or pseudo O_h coordination geometries). Third, in the 3:1 M^{n+} to polyoxoanion complexes, there is typically no further increase in the ~440 nm oxygen-to-metal charge-transfer band after the second equivalent of M^{n+} (e.g., see the Fe^{II} and Mn^{II} titrations in Figure 3a or the Cu^{II} titration in Figure 3b). This observation provides direct evidence that, in solution, the third equivalent of M^{n+} is only ion-paired to the polyoxoanion in these cases, $\{[(CH_3CN)_zM^{2+}][2(CH_3CN)_xM^{2+}]/P_2W_{15}Nb_3O_{62}^{9-}\}$ (M = Mn, Co, Fe), as opposed to having M^{n+} covalently and firmly bonded to the polyoxoanion. Ion-pairing interactions are precedented for $P_2W_{15}Nb_3O_{62}^{9-}$ specifically $Na^+\cdots P_2W_{15}Nb_3O_{62}^{9-}$ ion pairing off the polyoxoanion's C_3 symmetry axis which has been detected in solution by ^{31}P and ^{183}W NMR,[4a] and in the solid state by X-ray crystallography (see Figure 12 elsewhere[4c]).

Several points about the elemental analyses which follow will assist in understanding the results obtained and the present formulation of these complexes (all of which were dried at 40 °C and 10 mmHg overnight prior to their submission for elemental analysis). (i) The C/H/N ratios match those of the $n\text{-}Bu_4N^+$ countercations, strongly suggesting that all of the C/H/N is present as $n\text{-}Bu_4N^+$. [NMR analysis on the isolated and dried complexes confirms that the other possible C/H/N sources (CH_3CN, EtOAc, or Et_2O) are present only in trace amounts, much less than the amounts required to bring the calculated analyses into agreement with the found C/H/N values.] (ii) In the case of the complexes **2**, **4**, and **6**, the C/H/N analyses require the presence of *two additional (seven total) n-Bu4N+*, an unexpected result; this finding, in turn, requires the presence of two additional X^- anions (or one X^{2-} anion) as part of these complexes. In short, and although the analytical data require that ≥99% of the mass of these complexes is accounted for without the two X^- anions, the source of the two additional negative charges remains to be unequivocally identi-

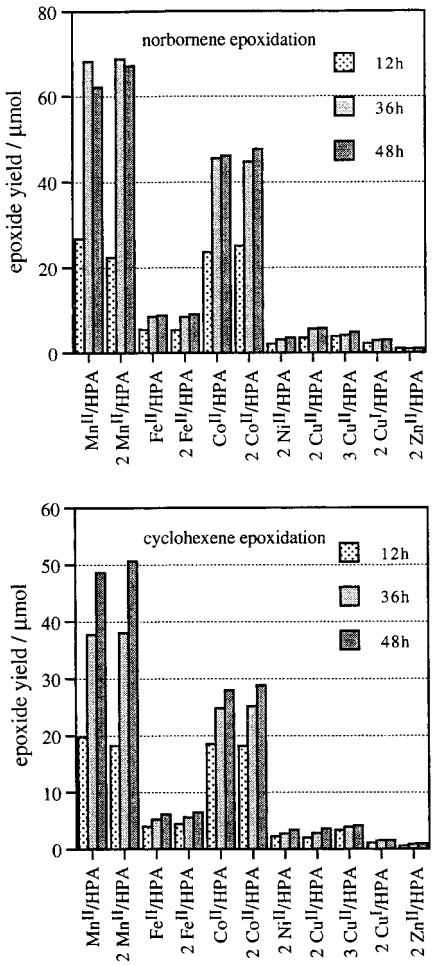

Figure 6. Comparison of catalytic efficiency (by total yields of epoxide in μmol after 12, 36, and 48 h, respectively) during epoxidation of norbornene (top), and cyclohexene (bottom), by $[PhIO]_n$ at 25 °C in acetonitrile under 1 atm N_2. The catalysts examined are the 11 different polyoxoanion-supported transition metal acetonitrile complexes, $\{m(CH_3CN)_xM^{n+}/P_2W_{15}Nb_3O_{62}^{9-}\}$ ($M^{n+} = Mn^{2+}$, Fe^{2+}, Co^{2+}, $m = 1$, 2; $M^{n+} = Cu^{2+}$, $m = 2$, 3; $M^{n+} = Ni^{2+}$, Zn^{2+}, Cu^{+}, $m = 2$). Ratios of catalyst/PhIO/substrate of approximately 1:80:95 were employed in all experiments.

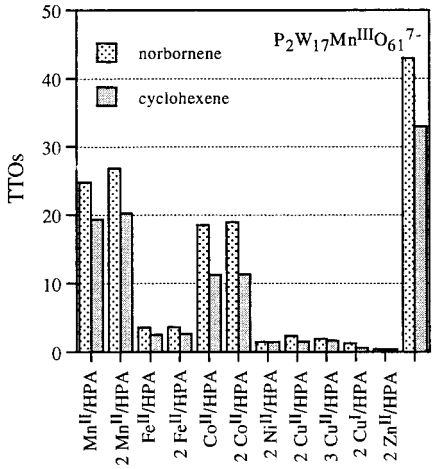

Figure 7. Comparison of catalytic total turnovers (TTO; per equivalent of catalyst obtained after 48 h) during epoxidation of norbornene (left columns) and cyclohexene (right columns) by $[PhIO]_n$ at 25 °C in acetonitrile under N_2. The catalysts examined are the 11 different polyoxoanion-supported transition metal acetonitrile complexes, $\{m(CH_3CN)_xM^{n+}/P_2W_{15}Nb_3O_{62}^{9-}\}$ ($M^{n+} = Mn^{2+}$, Fe^{2+}, Co^{2+}, $m = 1$, 2; $M^{n+} = Cu^{2+}$, $m = 2$, 3; $M^{n+} = Ni^{2+}$, Zn^{2+}, Cu^{+}, $m = 2$). For a comparison, the result obtained for norbornene epoxidation by the polyoxoanion-incorporated Mn^{III} complex, $P_2W_{17}Mn^{III}O_{61}^{7-}$, was added to this figure.

fied[34] (although 2 equiv of BF_4^-, or F^- from BF_4^- decomposition in the presence of electrophilic M(II), have been ruled out by B and F trace analyses).

Ion-Exchange Resin Experiments Demonstrating Inner-Sphere M^{n+} to Polyoxoanion Bonding. Evidence for the covalent, inner-sphere bonding within the best, $Mn(CH_3CN)_x^{2+}$ plus $P_2W_{15}Nb_3O_{62}^{9-}$ catalyst was obtained from experiments with ion-exchange resins. As detailed in the Experimental Section, in separate experiments acetonitrile solutions of $\{2(CH_3CN)_xMn^{2+}/P_2W_{15}Nb_3O_{62}^{9-}\}$ (**2**) were loaded onto a cation-exchange column in the *n*-Bu_4N^+ form, $P-SO_3^-$*n*-Bu_4N^+ (P = macroreticular polymer), and then slowly eluted down the column with CH_3CN. No retention of the purple, anionic $\{2(CH_3CN)_xMn^{2+}/P_2W_{15}Nb_3O_{62}^{9-}\}$ complex was observed. In a second series of experiments, **2** was loaded onto an anion-exchange column in its Cl^- form, $P-NR_3^+Cl^-$ (P = macroreticular polymer). Here the colored, anionic complex was completely retained on the column as expected. In separate control experiments, a solution of the acetonitrile complex, $[Mn(CH_3CN)_4](BF_4)_2$, in acetonitrile was loaded onto the same cation- and anion-exchange columns. As expected, the cationic $[Mn(CH_3CN)_4]^{2+}$ complex is retained on a cation-exchange colum but passes through the anion-exchange column. On the other hand, the 3:1 complex (3 $[Mn(CH_3CN)_4]^{2+}$ to 1

(34) (a) While the nature of the 2 "X^-" anion is uncertain at present, the only added (and thus deliberately present) anions are BF_4^- and $P_2W_{15}Nb_3O_{62}^{9-}$. However, ^{19}F NMR and trace B and F analyses (see the Supporting Information) show the presence of only trace BF_4^- ($\leq$0.5 equiv; and even though Mn·BF_4^- complexes are known[34b]), as well as no detectable F^- (i.e., from precedented BF_4^- decomposition[34c]), in the complexes purified by reprecipitation (**2**, **4**, and **6**−**11**); hence, the additional anion must derive, ultimately, from $P_2W_{15}Nb_3O_{62}^{9-}$. There are only two possibilities we can see, either (a) unprecedented (nonstoichiometric) compounds (e.g., the hypothetical "$[(n\text{-}Bu_4N)_7M^{II}_2][P_2W_{15}Nb_3O_{62}]_{1,22}$" or, equivalently, "$[(n\text{-}Bu_4N)_7M^{II}_2]_9[P_2W_{15}Nb_3O_{62}]_{11}$") or (b) $2X^- = 2OH^-$ anions (or conceivably a O^{2-} anion) made by reaction of trace H_2O with $P_2W_{15}Nb_3O_{62}^{9-}$ to give $H_2P_2W_{15}Nb_3O_{62}^{7-} + 2OH^-$. Note that the yields being $\leq$80% allow up to 20% of the added 1.0 equiv of the $P_2W_{15}Nb_3O_{62}^{9-}$ to be used in this fashion. A second, possible source of the putative OH^- is from a small excess of the $Bu_4N^+OH^-$ used in the preparation of the $P_2W_{15}Nb_3O_{62}^{9-}$. (We can rule out a two electron reduced, polyoxoanion-blue formulation for the extra 2^- charge, as the complexes are not blue, and also since the Nb^V-substituted $P_2W_{15}Nb_3O_{62}^{9-}$ polyoxoanion is very difficult to reduce; moreover, there is no potent enough, nor even sufficient quantity, reducing agent present, i.e., Fe(II) to Fe(III) cannot be the putative reducing agent.) *If* our present suspicion that the anion is $X^- = OH^-$ is correct, then it would follow that it might be in the form of "$Fe(OH)_2Fe$" supported atop the polyoxoanion, since bridging OH^- groups are well established for[34d] Fe^{II} and OH^- (and O^{2-} bridges are very common of course in Fe^{III} chemistry[34e,f]). Only strongly diffracting single crystals, and then X-ray crystallography, are likely to provide convincing proof for this tentative compositional and structural hypothesis in the present, very difficult case (since one is searching for hydroxy or oxo bridges in the presence of the many other oxos present in the pol*ox*oanion). Hence, crystallization trials are continuing. (b) Solid $[Mn(BF_4)]_x$ exhibiting Mn to BF_4^- bonding: Cockman, R. W.; Hoskins, B. F.; McCormick, M. J.; O'Donnell, T. A. *Inorg. Chem.* **1988**, *27*, 2742. The related solid $[Mn(AsF_6)]_x$: Borrmann, H.; Lutar, K.; Zemva, B. *Inorg. Chem.* **1997**, *36*, 880. (c) For F^- abstraction from BF_4^- or PF_6^- by electrophiles see p 929 and refs 21a,b,d−g in: Strauss, S. H. *Chem. Rev.* **1993**, *93*, 927. (d) Examples of complexes containing an $Fe^{II}(OH)_xFe^{II}$ moiety: Stassinopoulos, Schulte, G.; Papaefthymiou, G. C.; Cardonna, J. P. *J. Am. Chem. Soc.* **1991**, *113*, 8686 (see Figure 1 therein). (e) For examples of complexes containing an $Fe(X)_xFe$ moiety (X = O or OH), see Table 7 in: Wallar, B. J.; Lipscomb, J. D. *Chem. Rev.* **1996**, *96*, 2625. (f) $Fe^{III}(OH)_2Fe^{III}$ bridged polyoxoanions (with framework incorporated, as opposed to polyoxoanion-surface-supported, Fe^{III}): Zonnevijlle, F.; Tourné, C. M.; Tourné, G. F. *Inorg. Chem.* **1982**, *21*, 2751.

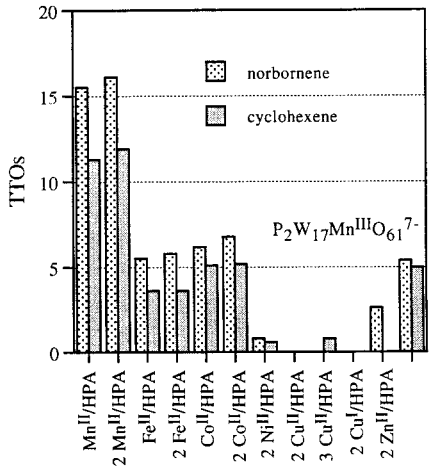

Figure 8. Comparison of catalytic total turnovers (TTO; per equivalent of catalyst obtained after 48 h) during epoxidation of norbornene (left columns) and cyclohexene (right columns) by $[PhIO]_n$ at 25 °C in dichloromethane under N_2. The catalysts examined are the 11 different polyoxoanion-supported transition metal acetonitrile complexes, $\{m(CH_3CN)_xM^{n+}/P_2W_{15}Nb_3O_{62}^{9-}\}$ ($M^{n+} = Mn^{2+}$, Fe^{2+}, Co^{2+}, $m = 1$, 2; $M^{n+} = Cu^{2+}$, $m = 2$, 3; $M^{n+} = Ni^{2+}$, Zn^{2+}, Cu^{+}, $m = 2$), as well as the polyoxoanion-incorporated Mn^{III} complex, $P_2W_{17}Mn^{III}O_{61}^{7-}$. It is worth noting two observations here: first, the total turnovers (TTOs) are lower in CH_2Cl_2 than in CH_3CN (Figure 7) and, second, the polyoxoanion-incorporated Mn^{III} complex is now less efficient than the supported $\{(CH_3CN)_xMn^{2+}/P_2W_{15}Nb_3O_{62}^{9-}\}$ (**1**) and $\{2(CH_3CN)_xMn^{2+}/P_2W_{15}Nb_3O_{62}^{9-}\}$ (**2**) complexes (where the opposite was true in CH_3CN). The lower $[PhIO]_n$ and catalyst solubility in CH_2Cl_2, compared to that in CH_3CN, provides an obvious rationalization for the lower TTOs in CH_2Cl_2. The explanation for the shift in reactivity of $\{(CH_3CN)_xMn^{2+}/P_2W_{15}Nb_3O_{62}^{9-}\}$ (**1**) and $\{2(CH_3CN)_xMn^{2+}/P_2W_{15}Nb_3O_{62}^{9-}\}$ (**2**) vs $P_2W_{17}Mn^{III}O_{61}^{7-}$ as a function of solvent is less clear, but may be due to *n*-Bu_4N^+ ion-pairing inhibition of the less accessible active site in $P_2W_{17}Mn^{III}O_{61}^{7-}$.

$P_2W_{15}Nb_3O_{62}^{9-}$) was prepared and examined in similar cation- and anion-exchange resin experiments (see the Experimental Section for details.) Here, the colored, anionic $\{3(CH_3CN)_xMn^{2+}/P_2W_{15}Nb_3O_{62}^{9-}\}$ complex is partly retained on both the cation- and anion-exchange columns. This is as expected if the third equivalent of $(CH_3CN)_xMn^{2+}$ is only ion-paired, but not covalently bound, to the polyoxoanion.

In summary, the ion-exchange experiments, as well as the oxygen-to-metal charge-transfer band and the M^{n+} to polyoxoanion stoichiometries obtained using this band, provide good evidence for the inner-sphere bonding of the first two equivalents of $Mn(CH_3CN)_x^{2+}$ to the $P_2W_{15}Nb_3O_{62}^{9-}$ polyoxoanion. Evidence for retention of this inner-sphere bonding of $Mn(CH_3CN)_x^{2+}$ to $P_2W_{15}Nb_3O_{62}^{9-}$ *after catalysis* is provided by analogous experiments, in addition to IR and UV−visible spectra, on the recovered catalyst (vide infra).

Results of Attempts To Grow Single Crystals for X-ray Crystallography. The presence of covalently attached 2:1 M^{II} to polyoxoanion complexes, and the possiblity of $M(X)_2M\cdot$ polyoxoanion structures ($M = Mn^{II}$, Fe^{II}, Co^{II}),[34] prompted attempts to grow single crystals for X-ray crystallography structural investigations. Unfortunately, our attempts to date to grow crystals suitable for X-ray diffraction have been unsuccessful, although our initial crystallization experiments have focused on the Zn^{2+} complex. Specifically, a less soluble mixed-cation[4c,d] *n*-Bu_4N^+/Na^+ salt was prepared of the Zn^{II} complex, $\{2(CH_3CN)_xZn^{2+}/P_2W_{15}Nb_3O_{62}^{9-}\}$, **11**. The mixed-cation *n*-Bu_4N^+/Na^+ complex of **11** was then used in multiple crystallization trials[35] using mixed solvents (acetonitrile, ethyl acetate, diethyl ether, tetrahydrofuran), as well as vapor diffusion (of ethyl acetate, diethyl ether, and tetrahydrofuran) into acetonitrile solutions of the complex at room temperature and at lower (0 to −20 °C) temperatures. In only four trials (vapor diffusion of diethyl ether into solutions of 25 mg of the Zn^{II} complex in 2 mL acetonitrile/ethyl acetate, 1:1) were microcrystals obtained; they proved, however, unsuitable for X-ray crystallography. A summary of additional crystallization trials is provided as Supporting Information. Attempts at crystallization of especially the 2 Mn^{II}, Fe^{II}, and Co^{II} complexes are continuing.

Evidence against the Formation of a $P_2W_{15}Nb_3O_{62}^{9-}$ Polyoxoanion-Stabilized, Colloidal $[MnO_x]$ Catalyst. We decided it would be prudent to test for the formation of polyoxoanion-stabilized $(MnO_x)_n$ colloids since $(MnO_x)_n$ colloids are known,[36] active oxidation catalysts,[37] and since $P_2W_{15}Nb_3O_{62}^{9-}$ is an excellent colloid stabilizer (albeit it of *uncharged*, *electrophilic* $M(0)_n$ particles,[38] but presumably not of any colloid with a surface anionic charge as $(MnO_x)_n$ might have). The single best and easiest way to identify such colloids is typically transmission electron microscopy (TEM),[39] authentic first-row transition-metal $M_xO_y(OH)_z$ colloids being readily visible by TEM, at least when present as larger particles.[40] Hence, a TEM image at 100−300 K magnification was obtained on samples of (a) the $\{2(CH_3CN)_xMn^{2+}/P_2W_{15}Nb_3O_{62}^{9-}\}$ (**2**) precursor (as a control) and (b) on a sample of the orange, gummy-solid catalyst after a cyclohexene/$[PhIO]_n$ oxidation run. The resultant TEMs, Figures S18 and S19, Supporting Information, show no signs of any nanocolloids. Hence, the rigorous conclusion here is that any particles present must be ≤10 Å. The catalyst isolation and spectroscopic reexamination studies described next provide confirming evidence that the true catalyst is not a colloid.

Catalyst Isolation and Reexamination after Use: IR, UV−Visible, and Ion-Exchange Evidence That the True Catalyst Is Polyoxoanion-Supported. Encouraged by the TEM studies above, and in order to provide what proved to be very strong evidence that the $\{2(CH_3CN)_xMn^{2+}/P_2W_{15}Nb_3O_{62}^{9-}\}$ (**2**) catalyst is polyoxoanion-supported, we scaled up a norbornene oxidation with $[PhIO]_n$ 4-fold, isolated the catalyst after 48 h of reaction time, and then examined the isolated catalyst by IR, UV−visible, and ion-exchange experiments, all in comparison to otherwise identical experiments on authentic **2** that had not been subjected to any catalysis. First, the isolated complex after catalysis was the same purple color *in solution* to the eye as the starting $\{2(CH_3CN)_xMn^{2+}/P_2W_{15}Nb_3O_{62}^{9-}\}$ (**2**). (Note that, as stated in the last section, the *solid* is orange, while in solution the isolated catalyst is purple.) Second, the IR and UV−visible of **2** before and after catalysis, Figures S20−S21 (Supporting Information), are virtually identical, providing very strong evidence that the supported polyoxoanion complex is the true catalyst. Third, experiments with ion-exchange resins show that the isolated purple complex after catalysis, and authentic **2**, both behave exactly as expected: both are retained on an anion-exchange column in its Cl^- form, $P-NR_3^+Cl^-$ (P

(35) The multiple countercations associated with polyoxometalate polyanions provide great flexibility in controlling their solubility properties by altering which cations are present. However, discovering which cation combinations give the desired properties is often experimentally tedious; see footnote 8 in: Edlund, D. J.; Saxton, R. J.; Lyon, D. K.; Finke, R. G. *Organometallics* **1988**, *7*, 1692.
(36) Perez-Benito, J. F.; Brillas, E.; Pouplana, R. *Inorg. Chem.* **1989**, *28*, 390.
(37) Perez-Benito, J. F.; Arias, C. *Int. J. Chem. Kinet.* **1991**, *23*, 717.
(38) (a) Aiken, J. D., III; Lin, Y.; Finke, R. G. *J. Mol. Catal.* **1996**, *114*, 29. (b) Lin, Y.; Finke, R. G. *J. Am. Chem. Soc.* **1994**, *116*, 8335.
(39) Lin, Y.; Finke, R. G. *Inorg. Chem.* **1994**, *33*, 4891.
(40) Matijević, E. *Acc. Chem. Res.* **1981**, *14*, 22.

Table 3. Epoxidation of *cis*-Stilbene in Acetonitrile with $[PhIO]_n$ as Oxidant[a] at 25 °C and under 1 atm Nitrogen Using the Mn^{II} Supported Catalysts $\{(CH_3CN)_xMn^{2+}/P_2W_{15}Nb_3O_{62}^{9-}\}$ (**1**), $\{2(CH_3CN)_xMn^{2+}/P_2W_{15}Nb_3O_{62}^{9-}\}$ (**2**), and the Polyoxoanion-Incorporated Analogue $P_2W_{17}Mn^{III}O_{61}^{7-}$

precatalyst	total turnovers	*cis*-/*trans*-epoxide ratio	*cis*-/*trans*-isomerization[b] (%)	benzaldehyde[b] (%)
$\{(CH_3CN)_xMn^{2+}/P_2W_{15}Nb_3O_{62}^{9-}\}$	20	0.68	4.8(±0.5)	37(±4)
$\{2(CH_3CN)_xMn^{2+}/P_2W_{15}Nb_3O_{62}^{9-}\}$	18	0.66	5.2(±0.5)	36(±4)
$P_2W_{17}Mn^{III}O_{61}^{7-}$	23	2.3	42(±4)	14(±1)

[a] Reaction conditions: acetonitrile, 3 mL; catalyst, 15 mg (ca. 2.5 μmol); $[PhIO]_n$, 21 mg (0.1 mmol); *cis*-stilbene, 33 mg (0.2 mmol); N_2; 24 h; 25 °C. GLC conditions: Carbowax; initial temperature, 100 °C; temperature-ramped 15°/min to a 250 °C final temperature; injector temperature, 200 °C; detector (FID) temperature, 200 °C. [b] Yield based on the limiting reagent $[PhIO]_n$.

= macroreticular polymer), while both purple complexes elute slowly with CH_3CN after being loaded (in separate experiments) onto a cation-exchange column in the *n*-Bu_4N^+ form, $P-SO_3^-$ *n*-Bu_4N^+ (P = macroreticular polymer; no retention of any of the purple color of $Mn^{II}_2{\cdot}P_2W_{15}Nb_3O_{62}^{9-}$ was observed in either case).

The above results provide excellent evidence that the true catalyst is polyoxoanion-supported Mn^{n+}, especially when combined with our finding that the rate of epoxidation is enhanced ≥14-fold in the presence of the polyoxoanion [which, in turn, requires that ≥93% of the catalysis (i.e., ≥93%/7% = 14) is due to $P_2W_{15}Nb_3O_{62}^{9-}$-supported Mn^{n+}]; moreover, there is presently no other precedented nor reasonable formulation of the catalyst that has not already been ruled out (e.g., the $M_xO_y(OH)_z$ colloid possiblity), at least that we can see. This is not to say, however, that additional catalyst characterization, and then kinetic and mechanistic studies, of this new subclass of polyxoanion-based oxidation catayst would not be of value.

Summary. Eleven new polyoxoanion-supported transition metal acetonitrile complexes have been prepared in 1:1, 1:2, and even 1:3 M^{n+} to polyoxoanion compositions; these new precatalysts were then tested for their catalytic efficacy for norbornene and cyclohexene oxygenation using $[PhIO]_n$ as the oxidant. The findings show a ca. 14-fold rate increase for $\{(CH_3CN)_xMn^{2+}/P_2W_{15}Nb_3O_{62}^{9-}\}$ (**1**) and $\{2(CH_3CN)_xMn^{2+}/P_2W_{15}Nb_3O_{62}^{9-}\}$ (**2**) in norbornene and cyclohexene epoxidation compared to the polyoxoanion-free $[Mn^{II}(CH_3CN)_4](BF_4)_2$, kinetic results which require the presence of the $P_2W_{15}Nb_3O_{62}^{9-}$ polyoxoanion in the rate-determining step and thus in the active catalyst. The catalytic epoxidation results identify the $\{(CH_3CN)_xMn^{2+}/P_2W_{15}Nb_3O_{62}^{9-}\}$ (**1**) and $\{2(CH_3CN)_xMn^{2+}/P_2W_{15}Nb_3O_{62}^{9-}\}$ (**2**) complexes as the best catalysts within this new subclass of polyoxoanion-supported catalysts. Catalyst isolation and then IR, UV−visible, and ion-exchange resin studies in comparison to authentic **2** provided further, seemingly compelling evidence that **2** is in fact the true catalyst. A comparison of **1** and **2** to the polyoxoanion-framework-incorporated $P_2W_{17}Mn^{III}O_{61}^{7-}$, the first such comparison of a polyoxoanion-supported and -incorporated catalyst, revealed evidence for the conceptual distinctiveness of these two types of polyoxoanion-based catalysts.

Overall, the key result is that another subclass of all-inorganic, oxidation-resistant, polyoxoanion-based catalysts is now available for catalytic survey, kinetic and, for the best and most interesting catalysts, full structural and mechanistic investigations. Single crystal X-ray structural studies of especially the novel 2:1 M^{II} to polyoxoanion complexes remain to be done and should prove of interest. Our recent discovery that there is record catalytic lifetime *dioxygenase* activity exhibited by related polyoxoanion-based precatalysts is noteworthy in this regard.[41]

Experimental Section

Materials. The metal acetonitrile complexes $[M^{n+}(CH_3CN)_y](BF_4)_n$ (M = Fe^{II}, Co^{II}, Ni^{II}, Mn^{II}, Zn^{II}, Cu^{II}, Cu^{I}) were prepared by the published procedures using the reaction of $NO^+BF_4^-$ and the M(0) powders in acetonitrile.[42] The copper(I) complex, $[Cu^I(CH_3CN)_4]BF_4$, was prepared by a modified, more recent method.[43] The acetonitrile complexes are hygroscopic and were, therefore, stored in a Vacuum Atmospheres drybox for the duration of this study. The compounds were analyzed by ICP analysis;[44,45] their purity was further confirmed by the absence of OH stretching bands (3000−4000 cm^{-1}) in their IR spectra (Nujol mulls). The triniobium-substituted Dawson polyoxoanion $(n\text{-}Bu_4N)_9P_2W_{15}Nb_3O_{62}$ was prepared on a 10 g scale according to our most recent literature procedures;[4e] care was taken to follow exactly the described synthesis and titration procedure with *n*-Bu_4NOH. The purity of the $(n\text{-}Bu_4N)_9P_2W_{15}Nb_3O_{62}$ was confirmed, in each batch prepared, by the observation of a clean ^{31}P NMR (CD_3CN; 14.3 mM; 22 °C; δ, number of P, $\Delta_{v1/2}$; −13.6, 1, $\Delta_{v1/2}$ = 1.2 ± 0.3 Hz; −6.6, 1, $\Delta_{v1/2}$ = 2.5 ± 0.3 Hz) and C,H,N analysis [% calcd (found); C, 27.57 (27.62); H, 5.21 (5.25); N, 2.01 (2.07)]. Moreover, if there was any question about the purity, a titration of the $(n\text{-}Bu_4N)_9P_2W_{15}Nb_3O_{62}$ with (1,5-COD)$Ir(CH_3CN)^{2+}$ was performed, a breakpoint at 1.0 ± 0.05 indicating that good, clean polyoxoanion had been prepared.[4e] $[PhIO]_n$ was *freshly pepared* by base hydrolysis of iodobenzene diacetate[46] (Aldrich) 1 day prior to use and stored in the Vacuum Atmospheres drybox. HPLC-grade solvents (ethyl acetate, dichloromethane, acetonitrile, and diethyl ether) were purchased from Aldrich and used as received. 1,2-Dichloroethane (Fisher Scientific) was used as received. Pyridine, 4-(*N*,*N*-dimethylamino)pyridine, and *N*-methylimidazole (Aldrich) were also used as received.

Instrumentation. The UV−visible spectra were recorded using a HP 8452A diode array system interfaced to IBM 486 computer. Infrared spectra were obtained on a Nicolet 5DX spectrometer as either KBr disks or as Nujol mulls. KBr (Aldrich, spectrophotometric grade) was used as received. All NMR spectra were obtained in Wilmad NMR tubes (5 mm o.d.) equipped with a J. Young valve, at room temperature unless otherwise stated. The chemical shifts are reported on the δ scale with downfield resonances as positive. ^{31}P NMR (121.5 MHz) spectra were recorded on a Bruker AC-300P NMR spectrometer and using a 33 mM CD_3CN solution (0.020 mmol of polyoxoanion in 0.6 mL of CD_3CN) unless otherwise stated. An external reference of 85% H_3PO_4 was used by the substitution method. Acquisition parameters are as follows: pulse width 5 μs, acquisition time 1.436 s, relaxation delay

(41) It is in developing robust, long-lived dioxygenase catalysts where our own present catalytic, structural, and kinetic and mechanistic investigations are focused: (a) Weiner, H.; Finke, R. G. *Inorg. Chim. Acta* **1999**, in press. (b) Weiner, H.; Finke, R. G. *J. Am. Chem. Soc.*, submitted.

(42) (a) Hathaway, B. J.; Holah, D. G.; Underhill, A. E. *J. Chem. Soc.* **1962**, 2444. (b) Hathaway, B. J.; Underhill, A. E. *J. Chem. Soc.* **1960**, 3705.

(43) (a) Kubas, G. J. *Inorg. Synth.* **1979**, *19*, 90. (b) Anderson, G. M.; Cameron, J. H.; Lappin, A. G.; Winfield, J. M. *Polyhedron* **1982**, *5*, 467−470.

(44) For ICP analysis of heteropolyoxoanions, see: Fernandez, M. A.; Bastiaans, G. J. *Anal. Chem.* **1979**, *51*, 1402.

(45) ICP atomic emission spectroscopy data for $[M^{n+}(CH_3CN)_m](BF_4)_n$ (M = Mn^{II}, Fe^{II}, Co^{II}, Ni^{II}, Cu^{II}, Cu^{I}, Zn^{II}); $Mn^{II}(CH_3CN)_6(BF_4)_2$ (MW, 392.7): Mn calcd. 14.9 (found 14.0). $Fe^{II}(CH_3CN)_6(BF_4)_2$ (MW, 475.7): Fe calcd 14.6 (found 13.4). $Co^{II}(CH_3CN)_6(BF_4)_2$ (MW 478.8): Co calcd 13.0 (found 12.3). $Ni^{II}(CH_3CN)_6(BF_4)_2$ (MW, 499.12): Ni calcd 11.8 (found 12.3). $Cu^{I}(CH_3CN)_4(BF_4)$ (MW, 314.5): Cu calcd 20.8 (found 20.2). $Cu^{II}(CH_3CN)_4(BF_4)_2$ (MW, 401.2): Cu calcd 15.8 (found 15.8). $Zn^{II}(CH_3CN)_6(BF_4)_2$ (MW 403.2): Zn calcd 17.6 (found 16.2).

(46) Sharefkin, J. G.; Saltzman, H. *Org. Synth., Coll. Vol.* **1973**, *5*, 660.

1.000 s, and sweep width 10 000 Hz. An exponential line broadening apodization (2.0 Hz) was applied to all spectra, but removed for any line widths reported. ^{19}F NMR (282.4 MHz) spectra were also recorded using a Bruker AC-300P NMR spectrometer and in 5 mm o.d. tubes. In all ^{19}F NMR measurements, a CD_3CN solution of 33 mM polyoxoanion and 28 mM (0.85 equiv) *n*-$Bu_4N^+PF_6^-$ as an internal standard was used. The PF_6^- resonance [= −72.3 ppm, referenced to neat $CFCl_3$ by the external substitution method, doublet, $^1J(^{31}P^{19}F) = 706$ Hz] was used as an internal standard both for chemical shifts and for quantitative analysis by integration of the signals [the number of fluorines, F, was calculated from the ratio of integrated intensities, with the knowledge that this −72.3 ppm signal (=0.85 equiv of PF_6^-) corresponds, therefore, to 5.1 F]. ^{19}F NMR acquisition parameters were as follows: pulse width 3.0 μs, acquisition time 0.623 s, relaxation delay 1.500 s, and sweep width 13 158 Hz (i.e., from −63 ppm to −155 ppm). An exponential line broadening apodization (1.5 Hz) was applied to all spectra, but removed for any line widths reported.

UV−Visible Titration of $(n\text{-}Bu_4N)_9P_2W_{15}Nb_3O_{62}$ with $[M^{n+}(CH_3CN)_y](BF_4)_n$ (M = Fe^{II}, Co^{II}, Ni^{II}, Mn^{II}, Zn^{II}, Cu^{II}, Cu^{I}). General Procedure. In a nitrogen atmosphere drybox, a solution of 31.36 mg (1.67 mM) of $(n\text{-}Bu_4N)_9P_2W_{15}Nb_3O_{62}$ in 3 mL of acetonitrile was prepared in a 5 mL vial and then placed in a 1 cm Schlenk cuvette (Pyrex glass), and the cell was septum capped. Next, 0.25 mL of a 0.15 M $[M^{n+}(CH_3CN)_y](BF_4)_n$ solution in acetonitrile ($[M^{n+}(CH_3CN)_y](BF_4)_n$, mg/1 mL of acetonitrile: Mn^{II}, 58.91 mg; Co^{II}, 71.83 mg; Fe^{II}, 71.36 mg; Ni^{II}, 74.87 mg; Cu^{II}, 60.20 mg; Cu^{I}, 47.18 mg; Zn^{II}, 60.48 mg) was prepared and transferred into a 250 μL syringe, and then transported outside of the drybox with the syringe needle stuck into a septa-capped vial. The titrations (see Figures S1−S4, Supporting Information) were accomplished by syringing 10 μL aliquots of the metal solvate solution into the cell followed by recording the UV−visible spectrum after each addition. No correction was made for the small, ≤8% total dilution effect during the titration. Addition of the concentrated metal solvate solution produced an initial precipitate of, presumably, an initial ion-pair (i.e., a noncovalent) adduct. This precipitate redissolved in a few seconds. [The solubility of this initial precipitate is dependent upon temperature and the concentration: addition of a more dilute, ca. 0.05 M metal solvate solution to the $(n\text{-}Bu_4N)_9P_2W_{15}Nb_3O_{62}$ polyoxoanion does prevent the precipitate from forming, but in turn provides too low an adsorption to allow quantitation of the titration by visible spectroscopy.]

Synthesis of the 1:1 Supported-Metal Solvates, $\{(CH_3CN)_yM^{2+}/P_2W_{15}Nb_3O_{62}^{9-}\}$ (M = Mn, Co, Fe). Following the 1:1 stoichiometries suggested by the UV−visible titrations (Figure 3a and Figure S2, Supporting Information), the three polyoxoanion-supported transition metal acetonitrile complexes $\{(CH_3CN)_xMn^{2+}/P_2W_{15}Nb_3O_{62}^{9-}\}$ (**1**), $\{(CH_3CN)_xCo^{2+}/P_2W_{15}Nb_3O_{62}^{9-}\}$ (**3**), and $\{(CH_3CN)_xFe^{2+}/P_2W_{15}Nb_3O_{62}^{9-}\}$ (**5**) were prepared as follows. In the drybox, 500 mg (0.08 mmol) of $(n\text{-}Bu_4N)_9P_2W_{15}Nb_3O_{62}$ was dissolved in 5 mL of HPLC-grade acetonitrile and placed in a 25 mL round-bottomed flask equipped with a 1 cm Teflon-coated magnetic stir bar. Then, 0.08 mmol of $[M^{n+}(CH_3CN)_y](BF_4)_n$ in 1 mL acetonitrile was added dropwise over 2 min to the clear solution,[47] resulting in a clear, homogeneous solution, and the reaction mixture was stirred for 2 h. The solvent was then evaporated in vacuo at room temperature, and the solids were dried at 40 °C and 10 mmHg for 24 h (the yields are quantitative). A comparison of the catalytic efficiencies of these complexes in the norbornene and cyclohexene epoxidation is provided in Tables 1 and 2 and Figures 6−8 (see also Table S1 and Figure S17 in the Supporting Information).

Synthesis of the 2:1 or 3:1 Supported-Metal Solvates, $\{m(CH_3CN)_yM^{2+}/P_2W_{15}Nb_3O_{62}^{9-}\}$ (M^{n+} = Mn^{2+}, Fe^{2+}, Co^{2+}, Ni^{2+}, Zn^{2+}, Cu^{+}, m = 2; M^{n+} = Cu^{2+}, m = 2, 3). Following the 2:1 or 3:1 stoichiometries observed by the UV−visible titrations (e.g., Figure 3 and Figures S3−S4, Supporting Information), eight polyoxoanion-supported transition metal acetonitrile complexes, $\{2(CH_3CN)_xMn^{2+}/P_2W_{15}Nb_3O_{62}^{9-}\}$ (**2**), $\{2(CH_3CN)_xCo^{2+}/P_2W_{15}Nb_3O_{62}^{9-}\}$ (**4**), $\{2(CH_3CN)_xFe^{2+}/P_2W_{15}Nb_3O_{62}^{9-}\}$ (**6**), $\{2(CH_3CN)_xNi^{2+}/P_2W_{15}Nb_3O_{62}^{9-}\}$ (**7**), $\{2(CH_3CN)_xCu^{2+}/P_2W_{15}Nb_3O_{62}^{9-}\}$ (**8**), $\{3(CH_3CN)_xCu^{2+}/P_2W_{15}Nb_3O_{62}^{9-}\}$ (**9**), $\{2(CH_3CN)_xCu^{+}/P_2W_{15}Nb_3O_{62}^{9-}\}$ (**10**), and $\{2(CH_3CN)_xZn^{2+}/P_2W_{15}Nb_3O_{62}^{9-}\}$ (**11**), were prepared as follows. All preparations were carried out in a nitrogen atmosphere drybox (<1 ppm oxygen). It is important to pay close attention to the exact details of the preparation which follows (specifically, the order of addition stated, and the use of the *exact* amounts and ratios of the solvents, CH_3CN and EtOAc, are crucial for the success of the synthesis). In the drybox, 500 mg (0.08 mmol) of $(n\text{-}Bu_4N)_9P_2W_{15}Nb_3O_{62}$ was dissolved in 5 mL of HPLC-grade acetonitrile and placed in a 25 mL round-bottomed flask equipped with a 1 cm Teflon-coated magnetic stir bar. Then, 0.16 mmol of $[M^{n+}(CH_3CN)_y](BF_4)_n$ (2:1 complexes) in 1 mL of acetonitrile (0.24 mmol for the 3:1 complexes) was added dropwise over 2 min to the clear solution,[48] resulting in a clear, homogeneous solution; the reaction mixture was then stirred for 2 h. After evaporation of the solvent in vacuo at room temperature, first 0.5 mL of acetonitrile and then 0.5 mL of HPLC-grade ethyl acetate were added; the resulting solution was clear and homogeneous. The mixture was then transferred with a plastic pipet into a 10 mL glass vial equipped with a 1 cm Teflon-coated magnetic stir bar. Next, 4 mL of HPLC-grade diethyl ether was added to the mixture under vigorous stirring, causing the formation of a fine (in some cases oily) precipitate. The crude material still contains ~0.4 equiv of *n*-$Bu_4N^+BF_4^-$ (by ^{19}F NMR, for the diamagnetic Zn^{II} complex, **11**, see Figure S8, Supporting Information). The crude product was then collected on a 15 mL medium glass frit and rinsed twice with 3 mL of ethyl acetate. The material was then redissolved in 0.5 mL of acetonitrile, and 0.5 mL of ethyl acetate was then added over 1 min with stirring. The solution was again clear and homogeneous. The desired product was then reprecipitated by adding the solution dropwise, using a plastic pipet and over ca. 2 min with vigorous stirring, to 60 mL of ethyl acetate. The suspension was stirred for 30 min, the precipitate was then collected on a 15 mL medium glass frit, redissolved again in 0.5 mL of acetonitrile and ethyl acetate, and the reprecipitation procedure was repeated. In each complex the final product was found to contains less than 0.5 equiv of *n*-$Bu_4N^+BF_4^-$ by ^{19}F NMR (<2.7% of the total mass); the spectrum for the diamagnetic Zn^{II} complex, **11**, is provided as Figure S8 of the Supporting Information. The trace amounts of BF_4^- were quantitatively confirmed by trace B and F elemental analyses in the case of **2**, **4**, and **6** (see the Supporting Information); those analytical results demonstrate that ^{19}F NMR and trace elemental analysis provide identical results within experimental error (and, hence, that the faster and cheaper ^{19}F NMR is the preferred method to check for residual BF_4^-, even in the presence of the paramagnetic metals such as in **2**, **4**, and **6**). Prior to sending for elemental analyses, the samples were dried at 40 °C and 10 mmHg for at least 24 h. The isolated yields for the eight polyoxoanion-supported transition-metal complexes are as follows (as crude materials; calculated for x = 0, at least in the solid state, and based on the elemental analyses of vacuum-dried samples): $\{2(CH_3CN)_xMn^{2+}/P_2W_{15}Nb_3O_{62}^{9-}\}$ (**2**), 386 mg (79%); $\{2(CH_3CN)_xCo^{2+}/P_2W_{15}Nb_3O_{62}^{9-}\}$ (**4**), 396 mg (76%); $\{2(CH_3CN)_xFe^{2+}/P_2W_{15}Nb_3O_{62}^{9-}\}$ (**6**), 421 mg (86%); $\{2(CH_3CN)_xNi^{2+}/P_2W_{15}Nb_3O_{62}^{9-}\}$ (**7**), 353 mg (76%); $\{2(CH_3CN)_xCu^{2+}/P_2W_{15}Nb_3O_{62}^{9-}\}$ (**8**), 325 mg (70%); $\{3(CH_3CN)_xCu^{2+}/P_2W_{15}Nb_3O_{62}^{9-}\}$ (**9**), 249 mg (55%); $\{2(CH_3CN)_xCu^{+}/P_2W_{15}Nb_3O_{62}^{9-}\}$ (**10**), 265 mg (53%); and $\{2(CH_3CN)_xZn^{2+}/P_2W_{15}Nb_3O_{62}^{9-}\}$ (**11**), 355 mg (82%).

Attempts To Grow Single Crystals for X-ray Crystallography. The details of these experiments are described in the Supporting Information.

Procedure for Norbornene Oxygenation Using $[PhIO]_n$ as Oxidant. Each reaction was carried out in a 5 mL vial inside the nitrogen atmosphere drybox and in HPLC-grade acetonitrile or dichloromethane. The mole ratio of catalyst/$[PhIO]_n$/substrate employed was 1:80:95. The catalyst (15 mg, ca. 2.5 μmol) and 48 mg (216 μmol; 80 equiv) of *freshly prepared* $[PhIO]_n$ were suspended in 2 mL of the HPLC-grade solvent, the $[PhIO]_n$ remaining largely insoluble as is well-

(47) The following amounts of $[M^{n+}(CH_3CN)_m](BF_4)_n$ complexes were dissolved in 1 mL of acetonitrile: Fe^{II}, 38.06 mg; Co^{II}, 38.31 mg; Mn^{II}, 31.42 mg.

(48) The following amounts of $[M^{n+}(CH_3CN)_m](BF_4)_n$ complexes were dissolved in 1 mL of acetonitrile: Fe^{II}, 76.12 mg (1:2); Co^{II}, 76.62 mg (2:1); Mn^{II}, 62.84 mg (2:1); Zn^{II}, 64.72 mg (1:2); Ni^{II}, 79.86 mg (1:2); Cu^{II}, 64.22 mg (2:1), 96.32 mg (1:3); Cu^{I}, 50.33 mg (1:2).

known. Next, 28 mg (215 μmol, ca. 95 equiv) of triply sublimed norbornene (Aldrich), dissolved in ca. 1 mL of acetonitrile, was syringed into the 5 mL vial to give 3 mL total volume and thereby start the reaction. The reaction vial was sealed using a rubber septum cap and Parafilm "M", and then stirred continuously for a total of 48 h with a 10 mm Teflon-coated magnetic stir bar. After 12, 36, and 48 h, 20 μL of reaction solution was transferred into a 3 mL vial; 1 mL of fresh solvent was then added and the sample was removed from the drybox. Next, 25 μL of an internal standard (cyclohexane, 231 μmol) was syringed in and the reaction mixture was analyzed by authentic-sample-calibrated GLC on a Carbowax capillary column (30 m length, 0.25 mm i.d.) using the following temperature program (which gave baseline resolution of the peaks; see Figure S14, Supporting Information): initial temperature, 50 °C (initial time, 3 min); heating rate, 10 °C/min; final temperature, 160 °C (final time, 5 min); injector temperature, 200 °C; FID detector temperature, 200 °C. A volume of 2 μL was injected.

Procedure for Cyclohexene Oxygenation Using $[PhIO]_n$ as Oxidant. All reactions were carried out in a 25 mL vial inside the nitrogen atmosphere drybox and in HPLC-grade acetonitrile or dichloromethane. The mole ratio of catalyst/$[PhIO]_n$/substrate employed was 1:65:200. The catalyst (15 mg, ca. 2.5 μmol) and 35 mg (158 μmol; ca. 65 equiv) of *freshly prepared* $[PhIO]_n$ were suspended in 5 mL of the HPLC-grade solvent, the $[PhIO]_n$ remaining largely insoluble as is well-known. Next, 50 μL (494 μmol, ca. 200 equiv) of freshly distilled cyclohexene (Aldrich, bp = 83 °C), dissolved in 1 mL solvent, was syringed into the 25 mL vial to give 6 mL total volume and thereby start the reaction. The reaction vial was sealed using a rubber septum cap and Parafilm "M", and then stirred continuously for a total of 48 h with a 10 mm Teflon-coated magnetic stir bar. After 12, 36, and 48 h, 20 μL of reaction solution was transferred into a 3 mL vial; 1 mL of fresh solvent was then added and the sample was removed from the drybox. Next, 10 μL of internal standard (cyclohexyl chloride, 85 μmol) was syringed in and the reaction mixture was analyzed by authentic-sample-calibrated GLC on the Carbowax capillary column previously cited (in the norbornene oxidation experimental section) and using the following temperature program (which gave baseline resolution of the peaks; see Figure S16 of the Supporting Information): initial temperature, 50 °C (initial time, 3 min); heating rate, 10 °C/min; final temperature, 160 °C (final time, 5 min); injector temperature, 200 °C; FID detector temperature, 200 °C. A volume of 2 μL was injected.

Procedure for *cis*-Stilbene Oxidation Stereochemical Studies. All reactions were carried out in a 5 mL vial inside the nitrogen atmosphere drybox. The mole ratio of catalyst/$[PhIO]_n$/substrate employed was 1:40:75. Catalyst (15 mg, ca. 2.5 μmol) and 21 mg (95 μmol; ca. 40 equiv) of freshly prepared $[PhIO]_n$ were suspended in 2 mL of HPLC-grade acetonitrile; then 33 mg (183 μmol; ca. 75 equiv) of *cis*-stilbene (Aldrich) dissolved in 1 mL acetonitrile was syringed into the 25 mL vial to give a final solution volume of 3 mL. The reaction was stirred inside the drybox for 24 h. The 25 mL vial was removed from the drybox, internal standard (cyclohexane; 5 μL, 46 μmol) was syringed in, and the reaction mixture was analyzed by GLC on the Carbowax capillary column previously cited (in the norbornene oxidation experimental section) and using the following temperature program (which provided baseline resolution of the key peaks; see Figure S15, Supporting Information): initial temperature, 100 °C (initial time, 0 min); temperature ramp, 15 °C/min; final temperature, 250 °C (final time, 10 min); injector temperature, 200 °C; FID detector temperature, 200 °C. A sample volume of 2 μL was injected. Note that the Carbowax column provides a clean separation of *cis*- and *trans*-stilbene oxide without any artifact peaks; however, a DB1 column showed an artifactual peak at 16.7 min (possibly the diol hydrolysis product of the epoxide) and, thus, a DB1 column should be avoided.

UV−Visible Titrations of Vacuum-Dried (n-Bu_4N)$_7$[Co^{II}/$P_2W_{15}Nb_3O_{62}$] (3) with Acetonitrile, Pyridine, *N*-(Dimethylamino)-pyridine, and *N*-Methylimidazole in 1,2-Dichloroethane. In a nitrogen atmosphere drybox, a 6.5 mM solution of $\{(CH_3CN)_xCo^{2+}/P_2W_{15}Nb_3O_{62}^{9-}\}$ (**3**) was prepared by dissolving 42.3 mg of vacuum-dried **3** in 3 mL of 1,2-dichloroethane using a 18 × 50 mm disposable glass vial. The clear, blue-green solution was then transferred into a 1 cm Schlenk cuvette (Pyrex glass) using a plastic pipet, and the cell was septum capped. In four independent experiments, separate 2 mL solutions were prepared: 1.12 M pyridine, 1.74 M acetonitrile, 1.24 M 4-(*N*,*N*-dimethylamino)pyridine, and 1.14 M *N*-methylimidazole, each in 1,2-dichloroethane. Then, 150 μL of each solution was transferred into a 250 μL syringe and brought outside of the drybox (the syringe needle was stuck into a septum-capped vial prior to removal). The titrations (see Figures S5−S7, Supporting Information) were accomplished by syringing 10 μL aliquots of the ligand solution into the cell, followed by recording of the UV−visible spectrum after each addition. (No correction was made for the small, ≤4% total dilution effect over the course of the titration.) The isolated $\{(CH_3CN)_xCo^{2+}/P_2W_{15}Nb_3O_{62}^{9-}\}$ (**3**) titrated with either CH_3CN or *N*-methylimidazole in 1,2-dichloroethane shows a break point at $x \approx 3$ equiv of CH_3CN or *N*-methylimidazole; hence, we have retained x (i.e., $x > 0$) in the above general formula, especially for the complexes in CH_3CN solution. Both pyridine and *N*-(dimethylamino)pyridine show approximate break points at 1 equiv of the pyridine ligand per equivalent of $\{(CH_3CN)_xCo^{2+}/P_2W_{15}Nb_3O_{62}^{9-}\}$ (**3**), an observation which was not investigated further but may be the result of the greater steric bulk of the pyridine ligands. Representative spectra are provided in the Supporting Information, Figures S5−S7.

TEM Experiments Probing for the Presence or Absence of a $(MnO_x)_n$ Colloid. Transmission electron microscopy (TEM) was performed using a JEOL 2000 EX-II 200 keV operating at an accelerating voltage of 100 keV. Samples were prepared using type A (300 mesh) Formvar and carbon-coated copper grids (Ted Pella). The grids were gently suspended in chloroform for about 30 s immediately prior to use to remove the Formvar coating and to expose a fresh carbon surface. The first grid was prepared by placing one drop of the polyoxoanion catalyst precursor $\{2(CH_3CN)_xMn^{2+}/P_2W_{15}Nb_3O_{62}^{9-}\}$ (**2**) (ca. 1 mg/mL in acetonitrile; Figure S18, Supporting Information) onto the grid and then allowing the grid to air-dry. The second grid was prepared by placing one drop of the catalyst and reaction solution containing **2** for 48 h in a norbornene oxygenation (ca. 1 mg/mL of catalyst in acetonitrile; Figure S19, Supporting Information), and then allowing it to air-dry. The samples were imaged by TEM at magnifications between 100 and 300 K, and in at least three different places on the sample grid to ensure that the images seen were representative for the whole sample.

Catalyst Reisolation after 48 h of Reaction Time of Norbornene Oxygenation. The reaction was carried out in a 25 mL vial inside the nitrogen atmosphere drybox in acetonitrile and at room temperature scaled up 4-fold vs that described in the section Procedure for Norbornene Oxidation Using $[PhIO]_n$ as Oxidant [$\{2(CH_3CN)_xMn^{2+}/P_2W_{15}Nb_3O_{62}^{9-}\}$, 60 mg; $[PhIO]_n$, 192 mg in 8 mL of CH_3CN; norbornene, 112 mg in 4 mL of CH_3CN]. The reaction mixture was stirred continuously for 48 h at room temperature, and the solvent was then removed by rotary evaporation. The residue was then extracted 4 times with 1 mL of CH_2Cl_2, the extracts were paper-filtered, and the filtrates were combined and evaporated to dryness. The purple-red solid was then washed 3 times with 1 mL of dry ethyl ether and dried overnight at 40 °C and in a vacuum (10 mmHg) to yield 50 mg of isolated catalyst.

Experiments Demonstrating Non-Ion-Exchangeability for 2 Before and After Oxidation Catalysis. All manipulations were performed outside of the drybox. Macroreticular, strongly acidic ion-exchange resin (5 g; Amberlyst 15; H^+ form; $P-SO_3H$) was placed in a beaker together with ca. 20 mL of degassed water. The resin was swirled for ca. 2 min, followed by removal of the water using a disposable plastic pipet. This process was repeated until the aqueous phase was clear and colorless. The resin was then packed onto a 36.5 cm × 1.2 cm (length × diameter) column. Next, 20 mL of degassed 40% n-$Bu_4N^+OH^-/H_2O$ was diluted to ca. 1 part in 10 with distilled water and then passed dropwise through the column. When the eluant tested basic with pH paper (S|P pH Indicator Strips, Baxter Diagnostics Inc.), distilled water was passed through the column until the eluant tested neutral with the same pH paper. The resultant $P-SO_3^-$ n-Bu_4N^+ column was then washed with four 25 mL portions of dry acetonitrile. A solution of ca. 50 mg of **2** in 1 mL of CH_3CN was then loaded onto the column. The purple solution was passed through the column dropwise with no apparent retention. The purple eluant was collected and the solvent removed by rotary evaporation under reduced pressure.

Then, 3.1 mg of the colored residue was dissolved in 10 mL of acetonitrile and the UV−visible spectrum was recorded between 200 and 500 nm (Figure S20, Supporting Information), demonstrating the presence of the polyoxoanion in the sample. A second, more concentrated sample (16.2 mg) was dissolved in 2 mL of acetonitrile, and the visible spectrum was recorded between 380 and 800 nm (Figure S20, Supporting Information), demonstrating that Mn^{II} is still bound to the polyoxoanion. In addition, the IR spectrum (KBr pellet) of 2 mg of the colored residue was recorded from 400 to 1200 cm^{-1} (Figure S21, Supporting Information), showing the characteristic pattern of the $\{2(CH_3CN)_xMn^{2+}/P_2W_{15}Nb_3O_{62}^{9-}\}$ complex (**2**).

An anion-exchange column of identical size was packed with strongly basic resin (Amberlyst A-27; Cl^- form; $P-NR_3^+Cl^-$) and was then washed with dry acetonitrile. A sample of **2** was loaded onto the column as described above for the cation-exchange resin. All of the purple sample was retained on the resin in the upper half of the column.

The experimental procedure described above for **2** was then repeated exactly only using 40 mg of the recovered catalyst from a catalytic norbornene oxidation with **2** as the catalyst (see the section just above, Catalyst Reisolation after 48 h of Norbornene Oxygenation). Non-ion-exchangeability, identical with that described above for authentic **2**, was found for the recovered catalyst material, demonstrating that $Mn(CH_3CN)_x^{2+}$ is not cleaved from the polyoxoanion support under the oxidation catalysis conditions applied in this study and even after 48 h of norbornene oxygenation catalysis. The superimposed UV−visible and IR spectra of **2**, vs those the recovered catalyst, are provided as Supporting Information, Figures S20−S21.

Acknowledgment. We thank Dr. Brian Arbogast, Department of Agricultural Chemistry, Oregon State University, Corvallis, OR, for making available to us the Kratos MS-50 mass spectrometer and carrying out the FAB-MS measurements. Financial support was provided by the National Science Foundation via Grant CHE 9531110.

Supporting Information Available: Details on UV−visible spectral titrations and their plots (7 pages); ^{19}F NMR spectroscopy showing that ≤0.15 equiv of BF_4^- remains in the reprecipitated Zn^{2+} complex, **11** (1 page); IR spectra of $\{2(CH_3CN)_xMn^{2+}/P_2W_{15}Nb_3O_{62}^{9-}\}$ (**2**), $\{2(CH_3CN)_xCo^{2+}/P_2W_{15}Nb_3O_{62}^{9-}\}$ (**4**), and $\{2(CH_3CN)_xFe^{2+}/P_2W_{15}Nb_3O_{62}^{9-}\}$ (**6**), IR data for the complexes **1**, **3**, **5**, **7**−**11**; elemental analysis data and interpretation; positive- and negative-ion FAB−MS spectra of the $\{2(CH_3CN)_xMn^{2+}/P_2W_{15}Nb_3O_{62}^{9-}\}$ (**2**), $\{2(CH_3CN)_xCo^{2+}/P_2W_{15}Nb_3O_{62}^{9-}\}$ (**4**), and $\{2(CH_3CN)_xFe^{2+}/P_2W_{15}Nb_3O_{62}^{9-}\}$ (**6**) complexes; summary of attempts to grow single crystals for X-ray crystallography; typical GLC charts for the norbornene, *cis*-stilbene, and cyclohexene epoxidations; a comparison of the catalytic efficacy of the "as isolated" and "as intentionally prepared" 1:1 and 2:1 M^{n+} to polyoxoanion complexes of Mn^{II}, Co^{II}, and Fe^{II} (2 pages); TEMs of the $\{2(CH_3CN)_xMn^{2+}/P_2W_{15}Nb_3O_{62}^{9-}\}$ (**2**) and its oxidation product (2 pages); and UV−visible and IR spectra for both the precatalyst **2** and a sample of **2** isolated after catalysis. This material is available free of charge via the Internet at http://pubs.acs.org.

IC990078K